A DISSERTATION FOR THE DEGREE OF DOCTOR OF PHILOSOPHY

Anthocyanin Biosynthesis Associated with Skin Coloration in Highbush Blueberry Fruit during Ripening

고관목 블루베리의 과실 성숙 중 과피 착색과 연관된 안토시아닌 생합성

BY

SUN WOO CHUNG

AUGUST, 2019

MAJOR IN HORTICULTURAL SCIENCE AND BIOTECHNOLOGY

DEPARTMENT OF PLANT SCIENCE

THE GRADUATE SCHOOL OF SEOUL NATIONAL UNIVERSITY

A DISSERTATION FOR THE DEGREE OF DOCTOR OF PHILOSOPHY

Anthocyanin Biosynthesis Associated with Skin Coloration in Highbush Blueberry Fruit during Ripening

고관목 블루베리의 과실 성숙 중 과피 착색과 연관된 안토시아닌 생합성

BY

SUN WOO CHUNG

AUGUST, 2019

MAJOR IN HORTICULTURAL SCIENCE AND BIOTECHNOLOGY

DEPARTMENT OF PLANT SCIENCE

THE GRADUATE SCHOOL OF SEOUL NATIONAL UNIVERSITY

Anthocyanin Biosynthesis Associated with Skin Coloration in Highbush Blueberry Fruit during Ripening

SUN WOO CHUNG

Major in Horticultural Science and Biotechnology
Department of Plant Science
The Graduate School of Seoul National University

ABSTRACT

Blueberry fruit accumulate high levels of anthocyanins with noticeable coloration process during ripening. For understanding anthocyanin biosynthesis associated with skin coloration during ripening, anthocyanin and anthocyanidin accumulation was monitored in 'Bluecrop' highbush blueberry fruit at three ripening stages, categorized based on fruit skin coloration: pale green at ca. 30 days after full bloom (DAFB), reddish purple at ca. 40 DAFB, and dark purple at ca. 50 DAFB. After the effects of abscisic acid (ABA) as a ripening signal were evaluated, transcriptional regulation of ABA biosynthesis, signal transduction, and anthocyanin biosyntehsis using transcripome analysis were also investigated at the three stages. Total anthocyanin contents increased during ripening, while fruit skin color steadily became darker and bluer, as reflected in decreasing L* (a color space coordinate describing lightness) and b* (describing blue-yellow coloration). Of the five anthocyanidins found in the fruit, cyanidin was first detected at the pale green

stage. Peonidin, delphinidin, petunidin, and malvidin were detected after the fruit had passed through the reddish purple stage. The contents of delphinidin and malvidin increased more rapidly than those of other anthocyanidins. All anthocyanidins detected were glycosylated with glucose, galactose, or arabinose. ABA application accelerated anthocyanin accumulation and fruit skin coloration, which provide the information that ABA can regulate anthocyanin biosynthesis during ripening. Transcriptome analysis revealed that 143 transcripts were annotated to encode five ABA biosynthesis enzymes, four ABA signal transduction regulators, four ABA-responsive transcription factors, and 12 anthocyanin biosynthesis enzymes. The analysis of differentially expressed genes between the ripening stages revealed that 11 transcripts, including those encoding nine-*cis*-epoxycarotenoid dioxygenase, SQUAMOSA-class MADS box transcription factor, and flavonoid 3',5'-hydroxylase, were significantly up-regulated throughout the entire ripening stages. In fruit treated with ABA, at least nine transcripts of these 11 transcripts as well as one transcript encoding flavonoid 3'-hydroxylase were up-regulated. These results showed the types and quantities of anthocyanidins, which in turn form anthocyanins, were correlated with changes in fruit skin color. They can also provide fundamental information demonstrating that ABA biosynthesis and signal transduction, and anthocyanin biosynthesis are closely associated with anthocyanin accumulation in highbush blueberry fruit during ripening.

Key words: abscisic acid, highbush blueberry, non-climacteric fruits, pigmentation, transcriptome analysis, *Vaccinium corymbosum*

Student number: 2009-21172

CONTENTS

LIST OF TABLES

LIST OF FIGURES

ABBREVIATIONS

AAO3	abscisic-aldehyde oxidase
ABA	abscisic acid
ABA2	xanthoxin dehydrogenase
ABF	abscisic acid-responsive element binding factor
ANOVA	analysis of variance
ANR	anthocyanidin reductase
ANS	anthocyanidin synthase
BCH	β-carotene 3-hydroxylase
bHLH	basic helix-loop-helix
c3g eq.	cyanidin 3-*O*-glucoside equivalent
CHI	chalcone isomerase
CHS	chalcone synthase
DAD	diode array detector
DAFB	days after full bloom
DAT	days after treatment
DFR	dihydroflavonol 4-reductase
F3H	flavanone 3-hydroxylase
F3’H	flavonoid 3’-hydroxylase
F3’5’H	flavonoid 3’,5’-hydroxylase
FPKM	fragments per kilobase of transcript per million mapped reads
FW	fresh weight
HPLC	high performance liquid chromatography
HSD	honest significant difference

LAR	leucoanthocyanidin reductase
MYB	myeloblastosis transcription factor
NCBI	National Center for Biotechnology Information
NCED	nine-*cis*-epoxycarotenoid dioxygenase
OMT	*O*-methyltransferase
PP2C	protein phosphatase 2C
PYL	pyrabactin resistance-like
PYR	pyrabactin resistance
RCAR	regulatory components of ABA recpetors
SnRK2	sucrose non-fermenting-1-related protein kinase 2
TDR	SQUAMOSA-class MADS box transcription factor
UFGT	anthocyanin 3-*O*-glucosyltransferase
UGT79B1	anthocyanidin 3-*O*-glucoside 2”’-*O*-xylosyltransferase
WDR	β-transduction repeat
ZEP	zeaxanthin epoxidase

GENERAL INTRODUCTION

Blueberry fruit are popular worldwide because of their flavor and abundant phytochemicals. Numerous studies have focused on their positive effects on human health (Gordillo et al., 2009; Lau et al., 2005). Blueberry fruit are one of the highest antioxidant capacities of any fruits or vegetables (Prior and Gu, 2005; Wu et al., 2006). The strong antioxidant capacity and health benefits are generally attributed to flavonoids including flavonols, anthocyanins, and proanthocyanidins. The anthocyanin content of blueberry fruit is considered of key importance because, as a visible flavonoid pigment, it can increase the commercial value, provide health benefits for humans, and protect the plant itself (Howard et al., 2003).

As the blueberry fruit undergo ripening, their skin color changes from pale green to purple or blue according to the accumulations of the individual anthocyanins derived from a particular anthocyanidin type (Zifkin et al., 2012). Pelargonidin, cyanidin, delphinidin, peonidin, petunidin, and malvidin are commonly found anthocyanidins in nature (Dudonné et al., 2015; Jaakola, 2013), but blueberry fruit contain five of these common anthocyanidins (all except pelargonidin), with the proportions varying across cultivars. Cyanidins, peonidins, and pelargonidins confer red colors, while delphinidins, petunidins, and malvidins are the main contributors of blue and purple colors (Hugueney et al., 2009). These anthocyanidins are glycosylated and also occur in acylated form, which stabilizes anthocyanins and enhances the colors (Giusti and Wrolstad, 2013).

Anthocyanins are biosynthesized via flavonoid pathway, which shares the same upstream with other flavonoids, including flavonols, flavanols, and proanythocyanidins, by sequential actions of enzymes and transcription factors

(Zifkin et al., 2012). Anthocyanin 3-*O*-glucosyltransferase (UFGT) is considered as the first key enzyme leading the flavonoid flux into the anthocyanin branch, although transcription factors are shared for biosynthesizing flavonoids (Lepiniec et al., 2006; Zifkin et al., 2012). Enzymes and transcription factors involved in anthocyanin biosynthesis have been investigated extensively at both the biochemical and genetic levels in several plants, including *Arabidopsis*, soybean, maize, and grape, but they have not well been studied in blueberry fruit.

The regulatory mechanism of anthocyanin biosynthesis is poorly understood, and little has been done to search for hormonal regulation (Jaakola, 2013). Especially, abscisic acid (ABA) is known as promoting anthocyanin biosynthesis during ripening of fruits in many plants including grape, strawberry (Jia et al., 2011), sweet cherry (Shen et al., 2014), bilberry (Karppinen et al., 2018), and blueberry fruits (Oh et al., 2018). In these fruits, a substantial rise in ABA content was accompanied at the onset of ripening with anthocyanin accumulation (Jia et al., 2011; Karppinen et al., 2018; Oh et al., 2018; Shen et al., 2014). ABA application in unripe fruits also enhanced anthocyanin accumulation with the skin coloration in grape (Roberto et al., 2012), strawberry (Jia et al., 2011), sweet cherry (Shen et al., 2014), bilberry (Karppinen et al., 2018), and blueberry fruits (Oh et al., 2018). Conversely, silencing of *nine-cis-epoxycarotenoid dioxygenase* (*NCED*), the limiting-step enzyme for ABA biosynthesis, showed anthocyanin-less phenotypes accompanied by the down-regulation of genes encoding anthocyanin biosynthesis enzyme in strawberry (Jia et al., 2011) and sweet cherry (Shen et al., 2014). However, the relationship between ABA signal transduction and anthocyanin biosynthesis during ripenig has been rarely studied.

In blueberry fruit, previous studies focused on identification and quantification

of individual anthocyanins in the fully ripe fruit (Ehlenfeldt and Prior, 2001; Kalt et al., 1999; Prior et al., 2001; Ribera et al., 2010). However, anthocyanin biosynthesis during ripening has rarely been studied. Blueberry fruit are suitable for studies of anthocyanin biosynthesis, because of highly noticeable coloration process with anthocyanin accumulation during ripening. The investigation of the regulatory mechanism can expand a view of the fruit ripening process involved in anthocyanin biosynthesis. In addition, it can provide genetic sources for breeding blueberries involved in improving fruit qualities and for a changing global environment.

In the present study, the types of anthocyanidin were quantified in correlation with fruit skin color. Anthocyanidin glycosylation patterns were investigated during ripening. To obtain an integrated view of the ripening process from ABA to anthocyanin biosynthesis, the transcriptomes of blueberry fruit were analyzed using RNA-Seq. The effects of ABA on anthocyanin accumulation and its regulatory transcript expression were also characterized.

LITERATURE REVIEW

Fruit coloration and anthocyanins

Anthocyanins, the most abundant and widespread flavonoid pigments, are responsible for red, purple, and blue colors in various plant organs (Lepiniec et al., 2006). In fruits, anthocyanins are the main factors to determine fruit quality. Diverse fruit colors depend on different types of anthocyanin, and their content levels (Jaakola, 2013).

Anthocyanins are glycosylated anthocyanidins with sugar moieties (Lepiniec et al., 2006). Variation in anthocyanin color results from the degrees of anthocyanidin hydroxylation and methoxylation (Jaakola, 2013). Most anthocyanins are derived from three types of anthocyanidins: pelargonidin, cyanidin, and delphinidin (Jaakola, 2013), with different numbers of hydroxyl groups on their B ring (Hugueney et al., 2009). An increase in the number of hydroxyl groups increases the blueness of anthocyanin. Methoxylation, which occurs on the C-3' or 5' hydroxyl groups, has a slight reddening effect (Hugueney et al., 2009). Thus, the fruit colors depend largely on the predominant type of anthocyanidin that forms anthocyanins. Six anthocyanidins, namely cyanidin, delphinidin, pelargonidin, peonidin, petunidin, and malvidin, occur generally in fruits (Jaakola, 2013). Glycosides of cyanidin and its methoxylated derivatives, peonidins and pelargonidins, confer red colors, while those of delphinidin and its methoxylated derivatives, petunidins and malvidins, are the main contributors of purple and blue colors (Lepiniec et al., 2006). Anthocyanin color intensity is enhanced by sugar moieties added (Jaakola, 2013). Most predominant anthocyanins are 3-*O*-glycosides, 5-*O*-glycosides, or 3,5-*O*-glycosides, in order of color intensity.

Glucose is most commonly attached, but other sugars as galactose, arabinose, xylose, and rhamnose are also present.

Anthocyanin biosynthesis

Anthocyanins are biosynthesized through the flavonoid pathway (Zifkin et al., 2012). The anthocyanin biosynthesis begins with the condensation of one molecule of 4-coumaroyl-coenzyme A and three molecules of malonyl-CoA, which results in naringenin chalcone. This reaction is conducted by chalcone synthase (CHS), before the pathway diverges into branches leading to various flavonoid classes, including flavonols, proanthocyanidins, and anthocyanins. Naringenin chalcone is converted to dihydrokaempferol by the sequential enzymatic actions of chalcone isomerase (CHI) and flavanone 3-hydroxylase (F3H). Flavonoid 3'-hydroxylase (F3'H) and flavonoid 3',5'-hydroxylase (F3'5'H) can then direct the route towards cyanidin and delphinidin anthocyanidins, respectively. The anthocyanidins are converted from leucoanthocyanins by anthocyanidin synthase (ANS) and further glycosylated by UFGT. Some of anthocyanins are methoxylated by *O*-methyltransferase (OMT).

Hormonal regulation and anthocyanin accumulation during ripening

Fruits are classified as climacteric or non-climacteric according to their ripening characteristics. At the onset of ripening, climacteric fruits, such as apple, banana, mango, and peach, display a concomitant burst of ethylene with well-characterized respiration peaks (Giovannoni, 2001). In contrast, non-climacteric fruits, including strawberry, grape, and blueberry, do not show the changes of ethylene contents and respiration (Frenkel, 1972), and ripening cannot be triggered by ethylene

application (Janes et al., 1978). However, the hormonal regulation of non-climacteric fruits ripening remains poorly understood.

ABA may be important in the ripening of some non-climacteric fruits, such as grape (Roberto et al., 2012), strawberry (Jia et al., 2011), and sweet cherry (Shen et al., 2014). In these fruits, ABA content increased at the onset of ripening with anthocyanin accumulation. Enhancement of anthocyanin accumulation by ABA application has also been observed in grape (Roberto et al., 2012), strawberry (Jia et al., 2011), and sweet cherry (Shen et al., 2014). These findings suggest that ABA is an essential role for anthocyanin biosynthesis during ripening. However, it is unclear whether these properties are shared by all non-climacteric fruits.

ABA biosynthesis

ABA belongs to a class of metabolites known as isoprenoids, also called terpenoids (Nambra and Marion-Poll, 2005). ABA is biosynthesized in the following three stages by the sequential actions of several classes of enzymes: (1) sequential modification of β-carotene by β-carotene 3-hydroxylase (BCH) and zeaxanthin epoxidase (ZEP), to ultimately produce violaxanthin; (2) conversion from violaxanthin to xanthoxin by NCED; and (3) biosynthesis of active ABA via xanthoxin dehydrogenase (ABA2) and abscisic-aldehyde oxygenase (AAO) (Nambra and Marion-Poll, 2005). The bioactive ABA undergoes hydroxylation and/or conjugation to produce non-bioactive catabolites, but these are reversible.

ABA signal transduction

Since ABA participates various plant development and stress responses, signal transduction is sophisticated with lots of components (Raghavendra et al., 2010).

Pyrabactin resistance/pyrabactin resistance1-like/regulatory components of ABA receptors (PYR/PYL/RCAR) constitute the initial step of the ABA signal transduction. They interact with protein phosphate 2C (PP2C) in an ABA-dependent manner to regulate the downstream activity of serin/threonine protein kinase of the sucrose non-fermenting related kinase 2 (SNRK2). In the absence of ABA, PP2C binds to the C termini of SnRK2 and block SnRK2 activity by removing phosphate groups from a region within the kinase domain termed the activation loop. Because the same domain of PP2C interacts with either the receptor or the kinase, these interactions are mutually exclusive for individual PP2C isoforms. ABA binding changes the conformation of PYR/PYL/RCAR to permit or enhance interaction with PP2C and thereby repress PP2C phosphate activity. This releases SnRK2 from inhibition. SnRK2 is then free to phosphorylate its many target proteins, including transcription factors that bind ABA-responsive element binding factor (ABF) to regulate the expression of ABA-responsive genes.

ABA-responsive transcription factors for anthocyanin biosynthesis

Although ABA signal transduction for biosynthesizing anthocyanins is not clear, some of ABA-responsive transcription factors involved in anthocyanin biosynthesis were discovered: MADS-box transcription factors (Jaakola, 2013) and the complex of myeloblastosis (MYB), basic helix-loop-helix (bHLH), and/or β-transduction repeat (WDR) transcription factors (Xu et al., 2015). Anthocyanin biosynthesis genes are known to be coordinately induced by the transcription factors that directly regulate the expression of genes encoding anthocyanin biosynthesis enzymes.

MADS-box genes are involved in controling all major aspects of development, including gametophyte development, embryo and seed development, as well as root,

flower and fruit development (Jaakola, 2013). In fruits, SQUAMOSA- and SEPALLATA-class MADS box genes are involved in the regulation of anthocyanin biosynthesis, although the links between the developmental regulatory factors and the downstream effectors involved in anthocyanin biosynthesis during ripening have not yet been unraveled. A link between anthocyanin biosynthesis and SQUAMOSA-class MADS box transcription factor *VmTDR4*, a homolog of the FRUITFULL in *Arabidopsis* and TDR4 in tomato, was reported in bilberry (Jaakola et al., 2010). Expression levels of *VmTDR4* were spatially and temporally consistent with anthocyanin accumulation in bilberry fruit and silencing of *VmTDR4* resulted in a substantial reduction of anthocyanin biosynthesis (Jaakola et al., 2010). Expression of the SEPALLATA-class MADS box transcription factor pyMADS18 was associated with anthocyanin accumulation in red and green forms of pear fruit (Wu et al., 2013).

In the complex of MYB, bHLH, and/or WDR, the expression pattern and the DNA-binding specificity of MYB and, to extent, bHLH also determine the subset of genes that are activated, whereas WDR seems to have a more general role in the regulatory complex (Xu et al., 2015). In *Arabidopsis* and grape fruit, some anthocyanin biosynthesis-related MYBs that are activated without bHLH or WDR have been identified (Jaakola, 2013).

MYB is involved in the regulation of the pathways of diverse secondary metabolites, signal transduction, developmental changes, and disease resistance (Azuma et al., 2015). *MYB* contains structurally conserved, 100 to 160 bp DNA-binding domains comprising single or multiple repeats. The R2R3MYB is most abundant among MYB class and some of this class are associated with the anthocyanin biosynthesis (Jaakola, 2013). Most of the MYB involved in the control

of anthocyanin biosynthesis are positive regulators that enhance the expression of the anthocyanin biosynthesis genes. However, repressors have also been characterized, such as FaMYB1 and VvMYB4 in strawberry (Aharoni et al., 2001) and grape fruits (Pérez-Díaz et al., 2016), respectively. bHLH and WDR involved in anthocyanin biosynthesis have been characterized in grape, apple, and strawberry fruits (Jaakola, 2013). In these fruits, the bHLH and WDR were shown to interact with different MYB proteins to induce promoters of anthocyanin biosynthesis genes. The bHLHs and MYB participating in the regulation of anthoyanin biosynthesis have been identified in maize, petunia, apple, grape, peach, and red rice (Xu et al., 2015).

LITERATURE CITED

Aharoni, A., C.H. De Vos, M. Wein, Z. Sun, R. Greco, A. Kroon, J.N. Mol, and A.P. O'Connell. 2001. The strawberry FaMYB1 transcription factor suppresses anthocyanin and flavonol accumulation in transgenic tobacco. Plant J. 28: 319–332.

Azuma, A., Y. Ban, A. Sato, A. Kono, M. Shiraishi, H. Yakushiji, and S. Kobayashi. 2015. MYB diplotypes at the color locus affect the ratios of tri/di-hydroxylated and methylated/non-methylated anthocyanins in grape berry skin. Tree Genet. Genom. 11: 1–13.

Dudonné, S., P. Dubé, F.F. Anhê, G. Pilon, A. Marette, M. Lemire, C. Harris, E. Dewailly, and Y. Desjardins. 2015. Comprehensive analysis of phenolic compounds and abscisic acid profiles of twelve native Canadian berries. J. Food Compos. Anal. 44: 214–224.

Ehlenfeldt, M.K. and R.L. Prior. 2001. Oxygen radical absorbance capacity (ORAC) and phenolic and anthocyanin concentrations in fruit and leaf tissues of highbush blueberry. J. Agric. Food. Chem. 49: 2222–2227.

Frenkel, C. 1972. Involvement of peroxidase and indole-3-acetic acid oxidase isozyme from pear, tomato, and blueberry fruits in ripening. Plant Physiol. 49: 757–763.

Giovannoni, J. 2001. Molecular biology of fruit maturation and ripening. Annu. Rev. Plant Physiol. Plant Mol. Biol. 52: 725–749.

Giusti, M.M. and R.E. Wrolstad. 2003. Acylated anthocyanins from edible sources and their applications in food systems. Biochem. Eng. J. 14: 217–225.

Gordillo, G., H. Fang, S. Khanna, J. Harper, G. Phillips, and C.K. Sen. 2009. Oral

administration of blueberry inhibits angiogenic tumor growth and enhances survival of mice with endothelial cell neoplasm. Antioxid. Redox. Signal. 11: 47–58.

Howard, L.R., J.R. Clark, and C. Brownmiller. 2003. Antioxidant capacity and phenolic content in blueberries as affected by genotype and growing season. J. Sci. Food Agric. 83: 1238–1247.

Hugueney, P., S. Provenzano, C. Verries, A. Ferrandino, E. Meudec, G. Batelli, D. Merdinoglu, V. Cheynier, A. Schuert, and A. Ageorges. 2009. A novel cation-dependent *O*-methyltransferase involved in anthocyanin methylation in grapevine. Plant Physiol. 150: 2057–2070.

Jaakola, L. 2013. New insights into the regulation of anthocyanin biosynthesis in fruits. Trends Plant Sci. 18: 447–483.

Jaakola, L., M. Poole, M.O. Jones, T. Kamarainen-Karppinen, J.J. Koskimaki, A. Hohtola, H. Haggman, P.D. Fraser, K. Manning, G.J. King, H. Thomson, and G.B. Seymour. 2010. A SQUAMOSA MADS box gene involved in the regulation of anthocyanin accumulation in bilberry fruits. Plant Physiol. 153: 1619–1629.

Janes, H.W., C.K. Chin, and C. Frenkel. 1978. Respiratory upsurge in blueberries and strawberries as influenced by ethylene and acetaldehyde. Bot. Gaz. 139: 50–52.

Jia, H.F., Y.M. Chai, C.L. Li, D. Lu, J.J. Luo, L. Qin, and Y.Y. Shen. 2011. Abscisic acid plays an important role in the regulation of strawberry fruit ripening. Plant Physiol. 157: 188–199.

Kalt, W., J.E. McDonald, R.D. Ricker, and X. Lu. 1999. Anthocyanin content and profile within and among blueberry species. Can. J. Plant Sci. 79: 617–623.

Karppinen, K., P. Tegelberg, H. Haggman, and L. Jaakola. 2018. Abscisic acid regulates anthocyanin biosynthesis and gene expression associated with cell wall modification in ripening bilberry (*Vaccinium myrtillus* L.) fruits. Front. Plant Sci. 9: 1259.

Lau, F.C., B. Shukitt-Hale, and J.A. Joseph. 2005. The beneficial effects of fruit polyphenols on brain aging. Neurobiol. Aging 26: 128–132.

Lepiniec, L., I. Debeaujon, J.M. Routaboul, A. Baudry, L. Pourcel, N. Nesi, and M. Caboche. 2006. Genetics and biochemistry of seed flavonoids. Annu. Rev. Plant Biol. 57: 405–430.

Nambra, E. and A. Marion-Poll. 2006. Abscisic acid biosynthesis and catabolism. Annu. Rev. Plant Biol. 56: 165–185.

Oh, H.D., D.J. Yu, S.W. Chung, S. Chea, and H.J. Lee. 2018. Abscisic acid stimulates anthocyanin accumulation in 'Jersey' highbush blueberry fruits during ripening. Food Chem. 244: 403–407.

Pérez-Díaz, J.R., J. Pérez-Díaz, J. Madrid-Espinoza, E. González-Villanueva, Y. Moreno, and S. Ruiz-Lara. 2016. New member of the R2R3-MYB transcription factors family in grapevine suppresses the anthocyanin accumulation in the flowers of transgenic tobacco. Plant Mol. Biol. 90: 63–76.

Prior, R.L. and L. Gu. 2005. Occurrence and biological significance of proanthocyanidins in the American diet. Phytochemistry 66: 2264–2280.

Prior, R.L., S.A. Lazarus, G. Cao, H. Muccitelli, and J.F. Hammerstone. 2001. Identification of procyanidins and anthocyanins in blueberries and cranberries (*Vaccinium* spp.) using high-performance liquid chromatography/mass spectrometry. J. Agric. Food Chem. 49: 1270–1276.

Raghavendra, A.S., V.J. Gonugunta, A. Christmann, and E. Grill. 2010. ABA

perception and signaling. Trends Plant Sci. 15: 395–401.

Ribera, A.E., M. Reyes-Diaz, M. Alberdi, G.E. Zuniga, and M.L. Mora. 2010. Antioxidant compounds in skin and pulp of fruits change among genotypes and maturity stages in highbush blueberry (*Vaccinium corymbosum* L.) grown in southern Chile. J. Soil Sci. Plant Nutr. 10: 509–536.

Roberto, S.R., A.M. Assis, L.Y. Yamamoto, L.C.V. Miotto, A.J. Sato, R. Koyama, and W. Genta. 2012. Application timing and concentration of abscisic acid improve color of 'Benitaka' table grape. Sci. Hortic. 142: 44–48.

Shen, X., K. Zhao, L. Liu, K. Zhang, H. Yuan, X. Liao, Q. Wang, X. Guo, F. Li, and T. Li. 2014. A role for PacMYBA in ABA-regulated anthocyanin biosynthesis in red-colored sweet cherry cv. Hong Deng (*Prunus avium* L.). Plant Cell Physiol. 55: 862–880.

Wu, J., G. Zhao, Y.N. Yang, W.Q. Le, M.A. Khan, S.L. Zhang, C. Gu, and W.J. Huang. 2013. Identification of differentially expressd genes related to coloration in red/green mutant pear (*Pyrus communis* L.). Tree Genet. Genom. 9: 75–83.

Wu, X., G.R. Beecher, J.M. Holden, D.B. Haytowitz, S.E. Gebhardt, and R.L. Prior. 2006. Concentrations of anthocyanins in common foods in the United States and estimation of normal consumption. J. Agric. Food Chem. 54: 4069–4075.

Xu, W., C. Dubos, and L. Lepiniec. 2015. Transcriptional control of flavonoid biosynthesis by MYB-bHLH-WDR complexes. Trends Plant Sci. 20: 176–185.

Zifkin, M., A. Jin, J.A. Ozga, L.I. Zaharia, J.P. Schernthaner, A. Gesell, S.R. Abrams, J.A. Kennedy, and C.P. Constabel. 2012. Gene expression and metabolite profiling of developing highbush blueberry fruit indicates transcriptional regulation of flavonoid metabolism and activation of abscisic acid metabolism. Plant Physiol. 158: 200–224.

CHAPTER I

Changes in Anthocyanidin and Anthocyanin Pigments in 'Bluecrop' Highbush Blueberry Fruit during Ripening

ABSTRACT

Accumulation of different types of anthocyanidins, in association with fruit skin coloration, was monitored in 'Bluecrop' highbush blueberry (*Vaccinium corymbosum* L.) at three stages of ripening: pale green at ca. 30 days after full bloom (DAFB); reddish purple at ca. 40 DAFB; and dark purple at ca. 50 DAFB. Total anthocyanin contents increased during ripening, while fruit skin color steadily became darker and bluer, as reflected in decreasing L* (a color space coordinate describing lightness) and b* (describing blue-yellow coloration). Of the six anthocyanidins commonly found in fruit, pelargonidin was absent throughout the ripening process. Cyanidin was first detected at the pale green stage. Peonidin, delphinidin, petunidin, and malvidin were detected after fruit had passed through the reddish purple stage. The contents of delphinidin and malvidin increased more rapidly than those of other anthocyanidins, and were closely correlated with changes in fruit skin color, demonstrating that the types and quantities of anthocyanidins, which in turn form anthocyanins, were major determinants of fruit skin coloration. Four anthocyanins were detected at the reddish purple stage, and 22 were identified at the dark purple stage. All anthocyanins detected were glycosylated with glucose, galactose, or arabinose.

Key words: anthocyanidins, anthocyanins, flavonoids, fruit pigmentation, fruit ripening, highbush blueberry, *Vaccinium corymbosum*

INTRODUCTION

Anthocyanins, the most abundant and widespread flavonoid pigments, are responsible for red, purple, and blue colors in diverse plant organs (Rowan et al., 2009; Yang et al., 2011). As non-toxic natural pigments, anthocyanins have been used to color processed foods instead of synthetic dyes (Veitch and Grayer, 2011). Anthocyanins are also well-known for their beneficial effects on human health, including protection from cancer, inflammation, heart disease, and other chronic diseases (Butelli et al., 2008; Xie et al., 2014). Anthocyanins are among the major factors determining quality in various fruits. Diverse fruit colors that depend on different types of anthocyanins, and their contents, have both commercial and aesthetic value (Liu et al., 2015).

Anthocyanins are glycosylated anthocyanidins with one or more sugar moieties. Variation in anthocyanin color results from the degrees of anthocyanidin hydroxylation and methoxylation (Azuma et al., 2015). Most anthocyanins are derived from three types of anthocyanidins: pelargonidin, cyanidin, and delphinidin (Jaakola, 2013; Fig. I-1), with different numbers of hydroxyl groups on their B ring (Hugueney et al., 2009). An increase in the number of hydroxyl groups increases the blueness of anthocyanin. Methoxylation, which frequently occurs on the C-3' and/or 5' hydroxyl groups (Fig. I-1), has a slight reddening effect (Hugueney et al., 2009). Thus, the colors of plant organs depend largely on the predominant type of anthocyanidin that forms anthocyanins. Quantification of anthocyanidins might be an efficient way of investigating the anthocyanin characteristics including color. Glycosides of cyanidin and its methoxylated derivatives, peonidins and pelargonidins, confer red colors, while those of delphinidin and its methoxylated

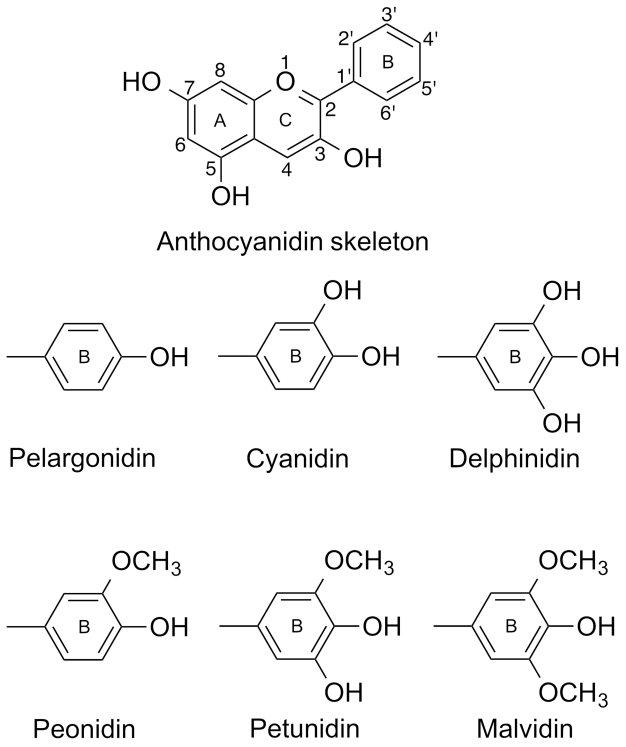

Fig. I-1. Anthocyanidin skeleton and the six most common anthocyanidins.

derivatives, petunidins and malvidins, are the main contributors of blue and purple colors (Hugueney et al., 2009).

Blueberry fruit are a good source of anthocyanins. During ripening, blueberry fruit change color from reddish purple to dark blue according to the accumulation of anthocyanins derived from a particular anthocyanidin type. Consumers prefer blueberry fruit with clearly distinct or dark color, because they believe that such fruit contain many compounds providing health benefits. Although anthocyanin accumulation has been characterized to relate to fruit skin coloration during ripening, individual anthocyanins, which can be measured by mass spectrometry, have not been quantified because of an absence of the respective standards.

In the present study, the contents of total anthocyanins, chlorophylls, and carotenoids associated with fruit skin coloration were monitored in 'Bluecrop' highbush blueberry (*Vaccinium corymbosum*) during ripening. Changes in anthocyanidins, rather than anthocyanins, were also monitored to quantify the predominant type of anthocyanidin in correlation with fruit skin color. In addition, anthocyanidin glycosylation patterns were investigated. The purposes of the present study are relevant to the establishment of a commercially valuable nutrient database related to fruit skin coloration, and health benefits.

MATERIALS AND METHODS

Plant materials

Ten-year-old highbush blueberry 'Bluecrop' highbush blueberry shrubs were grown in the experimental orchard of Seoul National University, Suwon (37° 17' N, 127° 00' E), Korea. Fruit ripening was categorized into three ripening stages based on their skin coloration: (1) pale green at ca. 30 days after full bloom (DAFB), (2) reddish purple at ca. 40 DAFB, and (3) dark purple at ca. 50 DAFB (Fig. I-2). Ninety fruit at each stage were harvested from three shrubs during ripening to provide three replicates with 30 fruit each in the sampling design. All harvested fruit were immediately frozen in liquid nitrogen and stored at –80°C until used.

Determination of fruit color

Fruit skin colors were measured using a spectrophotometer (CM-2500d; Minolta Co., Osaka, Japan) and described by the CIE L*, a*, and b* color space coordinates (McGuire, 1992). The L* value represents the lightness of colors, with a range of 0 to 100 (0, black; 100, white). The a* value is negative for green and positive for red. The b* value is negative for blue and positive for yellow. Hue angle (h°) and chroma (C*) were also calculated as $\tan^{-1}$ (b*/a*) and $(a^{*2} + b^{*2})^{1/2}$, respectively (McGuire, 1992). The parameter h° represents visual color appearance; 0°, red-purple; 90°, yellow; 180°, bluish-green; 270°, blue (McGuire, 1992). The parameter C* is the degree of departure from gray towards pure chromatic color; thus it represents color saturation or intensity (Little, 1975). For each fruit, the values were measured at three different points along the fruit equator.

Fig. I-2. Calyx end (top) and stem end (bottom) of ‘Bluecrop’ highbush blueberry fruit during ripening. Three ripening stages are based on skin coloration: pale green at ca. 30 days after full bloom (DAFB), reddish purple at ca. 40 DAFB, and dark purple at ca. 50 DAFB. Bar = 1 cm.

Determination of total anthocyanin content

Total anthocyanin content in whole fruit was determined by the pH differential method (Giusti and Wrolstad, 2001). Total anthocyanins were extracted separately in pH 1.0 and pH 4.5 buffers and then their absorbances were measured at 510 and 700 nm using a spectrophotometer (UV-Vis 2550, Shimadzu, Kyoto, Japan). Total anthocyanin content was calculated with the following equation:

Total anthocyanins (μg cyanidin 3-*O*-glucoside (c3g) equivalent (eq.) g^{-1} fresh weight (FW)) = $(A_{510} - A_{700})_{pH1.0} - (A_{510} - A_{700})_{pH4.5} \times 449.2/26{,}900 \times$ dilution factor

where 449.2 and 26,900 are the molecular mass and extinction coefficients of c3g, respectively.

Determination of total chlorophyll and carotenoid contents

Total chlorophyll and carotenoid contents in whole fruit were determined following the procedures of Lichtenthaler (1987). Absorbances of the extracts were measured at 661.6, 644.8, and 470 nm using a spectrophotometer (UV-Vis 2550, Shimadzu). Chlorophyll and carotenoid contents were calculated on the basis of μg g^{-1} FW using the following equations:

Chlorophyll a = $11.24\ A_{661.6} - 2.04\ A_{644.8}$

Chlorophyll b = $20.13\ A_{644.8} - 4.19\ A_{661.6}$

Total chlorophylls = $7.05\ A_{661.6} + 18.09\ A_{644.8}$

Total carotenoids = $(1{,}000\ A_{470} - 1.90$ chlorophyll a $- 63.14$ chlorophyll b$)/214$

Determination of individual anthocyanidin contents

Anthocyanins in whole fruit were hydrolyzed to anthocyanidins for extraction

following the procedures of Nyman and Kumpulainen (2001). The extracted anthocyanidins were separated in an XDB C-18 column (4.6 × 150.5 mm, 5 μm, Agilent, Santa Clara, CA, USA) equipped with a high performance liquid chromatography (HPLC) system (Ultimate 3000, Thermo Scientific, Waltham, MA, USA) fitted with a diode array detector (DAD) set at 520 nm. Eluents were passed through the column at a flow rate of 0.8 mL min^{-1} using a gradient of solvent A (aqueous 5% (v/v) formic acid) and solvent B (5% (v/v) formic acid in acetonitrile) in the following sequence: 0-50 min, 5-45% B; 50-55 min, 45% B; 55-58 min, 45-5% B; and 58-63 min, 5% B. Cyanidin, delphinidin, malvidin, pelargonidin (Sigma-Aldrich, St. Louis, MO, USA), peonidin (Santa Cruz Biotechnology, Dallas, TX, USA), and petunidin chlorides (Extrasynthese, Lyon, France) were used as standards.

Identification of individual anthocyanins

Individual anthocyanins in whole fruit were extracted using the procedures described by Wu and Prior (2005), and identified using a Q Exactive Hybrid Quadrupole-Orbitrap mass spectrometer (Thermo Scientific, Waltham, MA, USA) equipped with an HPLC system (Ultimate3000, Thermo Scientific) fitted with a DAD. An INNO 10 column (2.0 mm × 100 mm, 5 μm, Young Jin Biochrom, Seoul, Korea) was used for chromatographic separation. Anthocyanins were eluted using a gradient of mobile phase A (aqueous 5% (v/v) formic acid) and mobile phase B (5% (v/v) formic acid in acetonitrile) in the following sequence: 0-2 min, 10% B; 2-20 min, 10-20% B; 20-60 min, 20-30% B; 60-80 min, 30-40% B; 80-100 min, 40-80% B; 100-110 min, 80% B; 110-112 min, 80-10% B; and 112-120 min, 10% B. The flow rate was 1 mL min^{-1}; detections were made at 520 nm. Eluents were

ionized using an electrospray. The capillary temperature was maintained at 320°C, the ion source voltage was set at 3.5 kV, and the sheath and auxiliary gases were set at 30 and 5 units, respectively. The capillary voltage was set at 3.5 kV. The average scan time was 0.01 min, and the average time for changing polarity was 0.02 min. The energy of higher energy collision dissociation was generally chosen to maintain the precursor ion at about 30%. Identification and peak assignment of anthocyanins were based on comparisons of retention times and mass spectral data with published information (Gao and Mazza, 1995; Gavrilova et al., 2011; Prior et al., 2001; Wu and Prior, 2005).

Statistical analysis

Statistically significant differences were determined by analysis of variance (ANOVA) using the R 3.2.2 software package (http://www.r-project.org). Means were compared using the Tukey's honest significant difference (HSD) test at $P < 0.05$. Pearson correlation was used to quantify relationships between variables during ripening of blueberry fruit.

RESULTS AND DISCUSSION

Fruit skin coloration during ripening

L* and b* values of fruit skins steadily declined during ripening as the color became darker and bluer (Table I-1). The a* values, however, increased through the reddish purple stage, and then decreased slightly when the dark purple stage was reached. Fruit skins were mostly tinted red in the reddish purple stage. The reddening of fruit skin at the onset of ripening has also been observed in other fruits with dark blue or dark purple skins (Zifkin et al., 2012). Changes in fruit skin color during ripening (Fig. I-2) were also apparent in changes in h° values (Table I-1). The C* values decreased during ripening (Table I-1) as fruit skin colors became less vivid.

Pigment changes during ripening

The absence of anthocyanin in normally anthocyanin-rich fruits leads to the disappearance of fruit skin color, as in the white fruits of bilberry (*V. myrtillus*) and the diverse fruit color seen in mutated biotypes of the 'Sangiovese' grapevine (*Vitis vinifera*) (Jaakola et al., 2010; Ramazzotti et al., 2008). In the present study, the total anthocyanin contents increased steadily during ripening; they were 37-fold higher in the dark purple stage than in the pale green stage (Table I-2). However, total chlorophyll contents decreased steadily during ripening; total carotenoid contents insignificantly fluctuated, but remained relatively low. Rapid anthocyanin accumulation at the dark purple stage has been observed in fruit of other highbush blueberry cultivars, including 'Brigitta', 'Bluegold', and 'Legacy' (Ribera et al., 2010). Decreasing chlorophyll content is typical of ripening in many fruits (Guyer

Table I-1. Chromaticity values of 'Bluecrop' highbush blueberry fruit during ripening.

Ripening stage[1]	L*	a*	b*	h°	C*
Pale green	88.6 a[2]	−19.0 c	47.0 a	111.9 b	50.7 a
Reddish purple	74.8 b	19.3 a	16.4 b	40.3 c	25.8 b
Dark purple	51.1 c	2.3 b	−7.2 c	285.3 a	7.9 c

[1]Three ripening stages based on skin coloration: pale green at ca. 30 days after full bloom (DAFB), reddish purple at ca. 40 DAFB, and dark purple at ca. 50 DAFB.

[2]Means within columns followed by different letters are significantly different according to Tukey's HSD tests at $P < 0.05$.

Table I-2. Changes in anthocyanin, chlorophyll, and carotenoid contents of 'Bluecrop' highbush blueberry fruit during ripening.

	Total anthocyanin	Chlorophyll a	Chlorophyll b	Total chlorophyll	Total carotenoid
Ripening stage[1]	μg c3g eq. g^{-1} FW	μg g^{-1} FW			
Pale green	19.1 c[2]	48.3 a	11.5 a	59.8 a	0.6 a
Reddish purple	169.6 b	37.3 b	8.7 b	46.0 b	0.3 b
Dark purple	704.6 a	9.4 c	3.6 c	13.0 c	0.6 a

[1]Three ripening stages based on skin coloration: pale green at ca. 30 days after full bloom (DAFB), reddish purple at ca. 40 DAFB, and dark purple at ca. 50 DAFB.

[2]Means within columns followed by different letters are significantly different according to Tukey's HSD tests at $P < 0.05$.

et al., 2014) and low carotenoid content is common in blueberry fruit (Marinova and Ribarova, 2007). Total anthocyanin content of 'Bluecrop' fruit changed depending on growing region or cultivation method (Ehlenfeldt and Prior, 2001; Howard et al., 2003; Wang et al., 2008).

Anthocyanidin changes during ripening

Pelargonidin, cyanidin, delphinidin, peonidin, petunidin, and malvidin (Fig. I-1) are anthocyanidins commonly found in fruits (Jaakola, 2013). No pelargonidin was detected in any of the three stages in this study (Table I-3), thereby confirming that the absence of pelargonidin is a common characteristic of the fruits of the Ericaceae, including blueberry (Jaakola et al., 2002; Ribera et al., 2010)

Cyanidin was detected at the pale green stage (Table I-3, Fig. I-3). Cyanidin accumulation before ripening has been reported for 'Rubel' highbush blueberry fruit (Zifkin et al., 2012). Cyanidin contents decreased at the reddish purple stage as other anthocyanidins (delphinidin, peonidin, petunidin, and malvidin) accumulated (Table I-3, Fig. I-3). Malvidin was most abundant in this stage, followed by cyanidin, delphinidin, peonidin, and petunidin (Table I-3). Contents of all anthocyanidins identified in the reddish purple stage increased in the dark purple stage. Delphinidin and malvidin accumulated rapidly. Thus, delphinidin content was higher than cyanidin content in the dark purple stage (Table I-3). Petunidin was least abundant in both the reddish and dark purple stages (Table I-3). Similarly, delphinidin is the most abundant anthocyanidin in 'Rubel' highbush blueberry (Zifkin et al., 2012). However, in the dark purple stage of 'Bluetravel' and 'Ozarkblue' blueberry fruit, delphinidin was the least abundant anthocyanidin, and malvidin the most abundant (Oliveira et al., 2010). In the present study, 'Bluecrop'

Table I-3. Changes in anthocyanidin contents of 'Bluecrop' highbush blueberry fruit during ripening.

Ripening stage[1]	Pelargonidin	Cyanidin	Delphinidin	Peonidin	Petunidin	Malvidin
	μg g^{-1} FW					
Pale green	nd[2]	591 a[3]	nd	nd	nd	nd
Reddish purple	nd	190 b	99 b	66 b	6 b	315 b
Dark purple	nd	560 a	1,005 a	501 a	32 a	1,823 a

[1]Three ripening stages based on skin coloration: pale green at ca. 30 days after full bloom (DAFB), reddish purple at ca. 40 DAFB, and dark purple at ca. 50 DAFB.

[2]Not detected.

[3]Means within columns followed by different letters are significantly different according to Tukey's HSD tests at $P < 0.05$.

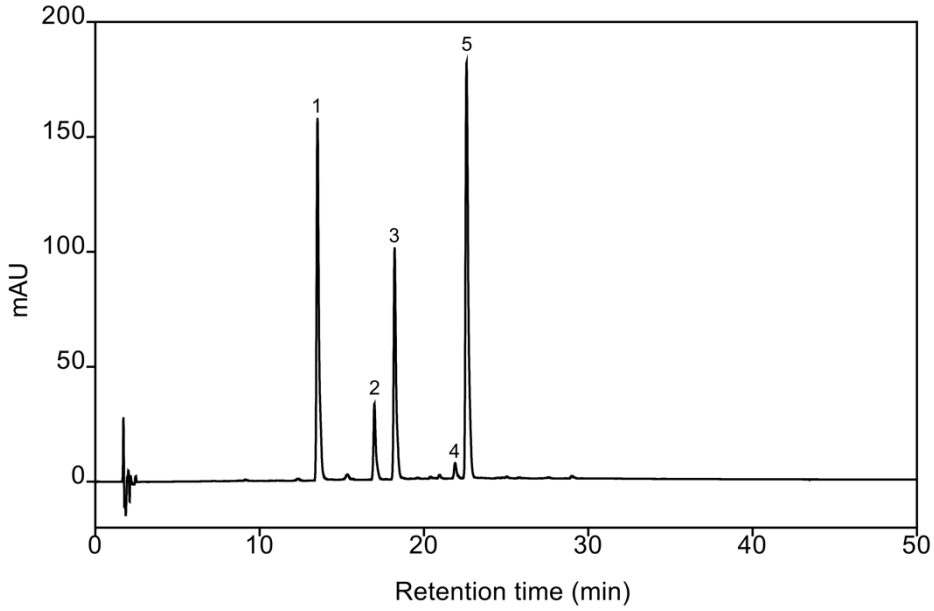

Fig. I-3. HPLC profile of anthocyanidins in 'Bluecrop' highbush blueberry fruit at dark purple stage (ca. 50 days after full bloom). 1, delphinidin; 2, cyanidin; 3, peonidin; 4, petunidin; 5, malvidin.

fruit accumulated more peonidin and malvidin (Table I-3) than ‘Rubel’ fruit (Zifkin et al., 2012). Thus, anthocyanidins with different degrees of hydroxylation and methoxylation accumulated differently, depending on the cultivar.

Anthocyanin changes during ripening

No anthocyanins were identified at the pale green stage (Table I-4), indicating that glycosylation had not occurred, and that the cyanidin identified at this stage (Table I-3) was only in the form of anthocyanidins. In the reddish purple stage, cyanidin and delphinidin were glycosylated with either galactose or arabinose (Table I-4). However, petunidin, peonidin, and malvidin had not been glycosylated in this stage, indicating that the accumulated forms (Table I-3) were anthocyanidins, and that methoxylation occurred prior to glycosylation. Glycosylation occurs prior to methoxylation at the onset of ripening; anthocyanidin glycosylation and subsequent methoxylation are coordinated by the activities of uridine diphosphate-glucose:flavonoid 3-*O*-glycosyltransferase and *O*-methyltransferase, respectively, which are only expressed during fruit ripening (Castellarin et al., 2011; Zifkin et al., 2012). Bailly et al. (1997) concluded that methoxylation occurs before acylation because *O*-methyltransferase is able to methoxylate cyanidin 3-*O*-glycosides, but has no catalytic activity on cyanidin 3-p-coumaroyl-*O*-glycosides. Methoxylation of the diverse forms of anthocyanidins does not commonly occur prior to glycosylation in higher plants (Lucker et al., 2010). Therefore, blueberry may have a unique pathway for anthocyanin biosynthesis. In the dark purple stage, all anthocyanidins were glycosylated with galactose, glucose, or arabinose (Table I-4, Fig. I-4); malvidin may also be glycosylated with xylose in this cultivar (Gavrilova et al., 2011). All of the anthocyanins identified in the present study were 3-*O*-

Table I-4. Anthocyanins identified in 'Bluecrop' highbush blueberry fruit during ripening

Peak	Retention time (min)	MS (*m/z*)	MS^2 (*m/z*)	Anthocyanin	Ripening stage[1]
1	25.4	465	303	delphinidin 3-*O*-galactoside	reddish purple, dark purple
2	28.0	465	303	delphinidin 3-*O*-glucoside	dark purple
3	30.3	449	287	cyanidin 3-*O*-galactoside	reddish purple, dark purple
4	32.0	435	303	delphinidin 3-*O*-arabinoside	reddish purple, dark purple
5	34.2	449	287	cyanidin 3-*O*-glucoside	dark purple
6	36.7	479	317	petunidin 3-*O*-galactoside	dark purple
7	37.9	419	287	cyanidin 3-*O*-arabinoside	reddish purple, dark purple
8	40.4	479	317	petunidin 3-*O*-glucoside	dark purple
9	42.5	463	301	peonidin 3-*O*-galactoside	dark purple
10	45.1	449	317	petunidin 3-*O*-arabinoside	dark purple

Table I-4. Continued.

Peak	Retention time (min)	MS (*m/z*)	MS^2 (*m/z*)	Anthocyanin	Ripening stage
11	47.3	463	301	peonidin 3-*O*-glucoside	dark purple
12	48.4	493	331	malvidin 3-*O*-galactoside	dark purple
13	52.5	463	331	malvidin 3-*O*-arabinoside	dark purple
14	57.6	535	287	cyanidin 3-*O*-(malonyl)glucoside	dark purple
15	64.4	491	287	cyanidin 3-*O*-(6”-acetyl)galactoside	dark purple
16	67.3	507	331	delphinidin 3-*O*-(6”-acetyl)glucoside	dark purple
17	74.8	505	303	peonidin 3-*O*-(6”-acetyl)galactoside	dark purple
18	75.6	491	287	cyanidin 3-*O*-(6”-acetyl)glucoside	dark purple
19	76.9	535	331	malvidin 3-*O*-(6”-acetyl)galactoside	dark purple
20	78.6	521	317	petunidin 3-*O*-(6”-acetyl)glucoside	dark purple
21	83.9	505	301	peonidin 3-*O*-(6”-acetyl)glucoside	dark purple

Table I-4. Continued.

Peak	Retention time (min)	MS (m/z)	MS^2 (m/z)	Anthocyanin	Ripening stage
22	85.3	535	331	malvidin 3-*O*-(6”-acetyl)glucoside	dark purple

Peak numbers and retention time correspond to Fig. I-4.

[1]Three ripening stages based on skin coloration: pale green at ca. 30 days after full bloom (DAFB), reddish purple at ca. 40 DAFB, and dark purple at ca. 50 DAFB.

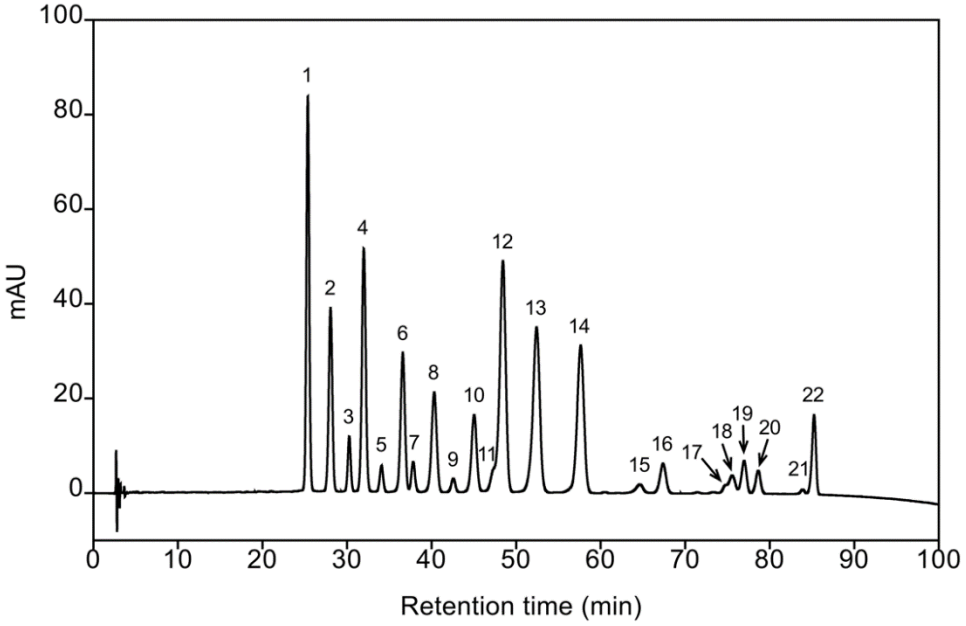

Fig. I-4. HPLC profile of anthocyanins in 'Bluecrop' highbush blueberry fruit at dark purple stage (ca. 50 days after full bloom). 1, delphinidin 3-*O*-galactoside; 2, delphinidin 3-*O*-glucoside; 3, cyanidin 3-*O*-galactoside; 4, delphinidin 3-*O*-arabinoside; 5, cyanidin 3-*O*-glucoside; 6, petunidin 3-*O*-galactoside; 7, cyanidin 3-*O*-arabinoside; 8, petunidin 3-*O*-glucoside; 9, peonidin 3-*O*-galactoside; 10, petunidin 3-*O*-arabinoside; 11, peonidin 3-*O*-glucoside; 12, malvidin 3-*O*-galactoside; 13, malvidin 3-*O*-arabinoside; 14, cyanidin 3-*O*-(malonyl)glucoside; 15, cyanidin 3-*O*-(6"-acetyl)galactoside; 16, delphinidin 3-*O*-(6"-acetyl)glucoside; 17, peonidin 3-*O*-(6"-acetyl)galactoside; 18, cyanidin 3-*O*-(6"-acetyl)glucoside; 19, malvidin 3-*O*-(6"-acetyl)galactoside; 20, petunidin 3-*O*-(6"-acetyl)glucoside; 21, peonidin 3-*O*-(6"-acetyl)glucoside; 22, malvidin 3-*O*-(6"-acetyl)glucoside.

monoglycosides (Table I-4). Anthocyanin 5-*O*-glycosides, di-*O*-glycosides, and tri-*O*-glycoides have not been identified in blueberry fruit (Wu and Prior, 2005).

Acylated anthocyanins, with acetyl or malonyl groups, were also detected when glycosylation occurred with galactose or glucose, but not with arabinose (Table I-4), as reported previously (Gavrilova et al., 2011; Prior et al., 2001). However, anthocyanin acylation with a malonyl group was detected only in cyanidin 3-*O*-glucoside (Table I-4). Aromatic or aliphatic acylation of some anthocyanins provides fruits with more intense colors (Zhang et al., 2014). Aromatic acylation induces intramolecular stacking of the anthocyanins with polyphenols, resulting in bluer coloration and more stable structures; aliphatic acylation enhances water solubility of the anthocyanins and protects their glycosides from enzymatic degradation (Zhang et al., 2014).

Correlation between skin coloration and pigments

Changes in the anthocyanidins and anthocyanins in 'Bluecrop' highbush blueberry fruit during ripening were significantly correlated with skin coloration (Table I-5). Total anthocyanin and chlorophyll contents were correlated with L*, b*, h°, and C*, but total carotenoid content was not correlated with any color parameters. Correlation coefficients for relationships of individual anthocyanidins with chromaticity values confirmed that anthocyanin accumulation in terms of anthocyanidin type was the major determinant of fruit skin coloration. Among anthocyanidins, delphinidin and malvidin were most strongly correlated with four chromaticity values, but not L*. Cyanidin rarely had any effect on fruit skin coloration during ripening. Accumulations of delphinidin and malvidin may result in shifts of the visible absorption maximum towards a bluer hue (Giusti and

Table I-5. Correlation coefficients for the relationships of pigments and chromaticity values of 'Bluecrop' highbush blueberry fruit.

Variable	L*	a*	b*	h°	C*
Cyanidin	−0.20^{ns}	−0.76***	0.13^{ns}	0.64*	0.16^{ns}
Peonidin	−0.58*	−0.80***	−0.86***	0.80***	−0.84**
Delphinidin	−0.62^{ns}	−0.92***	−0.94***	0.94***	−0.92***
Petunidin	−0.51*	−0.87***	−0.77**	0.82**	−0.88***
Malvidin	−0.47*	−0.93***	−0.95**	0.95***	−0.92***
Total anthocyanin	−0.84***	0.26^{ns}	−0.88***	0.87***	−0.85***
Total chlorophyll	0.89***	−0.32^{ns}	0.87***	−0.82***	0.83***
Chlorophyll a	0.86***	−0.30^{ns}	0.87***	−0.82***	0.84***
Chlorophyll b	0.85***	−0.32^{ns}	0.78***	−0.73**	0.75**
Total carotenoid	0.04^{ns}	−0.25^{ns}	−0.10^{ns}	0.35^{ns}	−0.15^{ns}

^{ns,*,**,***} Non-significant or significant at $P < 0.05$, 0.01, or 0.001, respectively.

Wrolstad, 2003).

In conclusion, fruit skin color of ‘Bluecrop’ highbush blueberry may be determined by the types and quantities of anthocyanins, derived from the predominant types of anthocyanidins. Since delphinidin and its methoxylated derivative, malvidin, were the major anthocyanidins, their glycosides may be the main contributors to fruit skin coloration, as indicated by the color changes from pale green to dark purple.

LITERATURE CITED

Azuma, A., Y. Ban, A. Sato, A. Kono, M. Shiraishi, H. Yakushiji, and S. Kobayashi. 2015. MYB diplotypes at the color locus affect the ratios of tri/di-hydroxylated and methylated/non-methylated anthocyanins in grape berry skin. Tree Genet. Genom. 11: 1–13.

Bailly, C., F. Cormier, and C.B. Do. 1997. Characterization and activities of *S*-adenosyl-L-methionine:cyanidin 3-glucoside 3'-*O*-methyltransferase in relation to anthocyanin accumulation in *Vitis vinifera* cell suspension cultures. Plant Sci. 122: 81–89.

Butelli, E., L. Titta, M. Giorgio, H.P. Mock, A, Matros, S. Peterek, E.G.W.M. Schijlen, R.D. Hall, A.G. Bovy, J. Luo, and C. Martin. 2008. Enrichment of tomato fruit with health-promoting anthocyanins by expression of select transcription factors. Nat. Biotechnol. 26: 1301–1308.

Castellarin, S.D., G.A. Gambetta, H. Wada, K.A. Shackel, and M.A. Matthews. 2011. Fruit ripening in *Vitis vinifera*: spatiotemporal relationships among turgor, sugar accumulation, and anthocyanin biosynthesis. J. Exp. Bot. 62: 4345–4354.

Ehlenfeldt, M.K. and R.L. Prior. 2001. Oxygen radical absorbance capacity (ORAC) and phenolic and anthocyanin concentrations in fruit and leaf tissues of highbush blueberry. J. Agric. Food. Chem. 49: 2222–2227.

Gao, L. and G. Mazza. 1995. Characterization of acetylated anthocyanins in lowbush blueberries. J. Liq. Chromatogr. 18: 245–259.

Gavrilova, V., M. Kajdzanoska, V. Gjamovski, and M. Stefova. 2011. Separation, characterization, and quantification of phenolic compounds in blueberries and red and black currants by HPLC-DAD-ESI-MS^n. J. Agric. Food Chem. 59:

4009–4018.

Giusti, M.M. and R.E. Wrolstad. 2001. Characterization and measurement of anthocyanins by UV-visible spectroscopy. In Wrolstad R.E., T.E. Acree, E.A. Decker, M.H. Penner, D.S. Reid, S.J. Schwartz, C.F. Shoemaker, D.M. Smith, and P. Sporns, eds., Current Protocols in Food Analytical Chemistry. John Wiley & Sons, New York, NY, USA, pp 1.2.1–1.2.13

Giusti, M.M. and R.E. Wrolstad. 2003. Acylated anthocyanins from edible sources and their applications in food systems. Biochem. Eng. J. 14: 217–225.

Guyer, L., S.S. Hofstetter, B. Christ, B.S. Lira, M. Rossi, and S. Hortensteiner. 2014. Different mechanisms are responsible for chlorophyll dephytylation during fruit ripening and leaf senescence in tomato. Plant Physiol. 166: 44–56.

Howard, L.R., J.R. Clark, and C. Brownmiller. 2003. Antioxidant capacity and phenolic content in blueberries as affected by genotype and growing season. J. Sci. Food Agric. 83: 1238–1247.

Hugueney, P., S. Provenzano, C. Verries, A. Ferrandino, E. Meudec, G. Batelli, D. Merdinoglu, V. Cheynier, A. Schubert, and A. Ageorges. 2009. A novel cation-dependent *O*-methyltransferase involved in anthocyanin methylation in grapevine. Plant Physiol. 150: 2057–2070.

Jaakola, L. 2013. New insights into the regulation of anthocyanin biosynthesis in fruits. Trends Plant. Sci. 18: 477–483.

Jaakola, L., K. Maatta, A.M. Pirttila, R. Torronen, S. Karenlampi, and A, Hohtola. 2002. Expression of genes involved in anthocyanin biosynthesis in relation to anthocyanin, proanthocyanidin, and flavonol levels during bilberry fruit development. Plant Physiol. 130: 729–739.

Jaakola, L., M. Poole, M.O. Jones, T. Kamarainen-Karppinen, J.J. Koskimaki, A.

Hohtola, H. Haggman, P.D. Fraser, K. Manning, G.J. King, H. Thomson, and G.B. Seymour. 2010. A SQUAMOSA MADS box gene involved in the regulation of anthocyanin accumulation in bilberry fruits. Plant Physiol. 153: 1619–1629.

Lichtenthaler, H.K. 1987. Chlorophylls and carotenoids: pigments of photosynthetic biomembranes. Methods Enzymol. 148: 350–382.

Little, A.C. 1975. Off on a tangent. J. Food Sci. 40: 410–411.

Liu, T., S. Song, Y. Yuan, D. Wu, M. Chen, Q. Sun, B. Zhang, C. Xu, and K. Chen. 2015. Improved peach peel color development by fruit bagging: enhanced expression of anthocyanin biosynthetic and regulatory genes using white non-woven polypropylene as replacement for yellow paper. Sci. Hortic. 184: 142–148.

Lucker, J., S. Martens, and S.T. Lund. 2010. Characterization of a *Vitis vinifera* cv. Cabernet Sauvignon 3',5'-*O*-methyltransferase showing strong preference for anthocyanins and glycosylated flavonols. Phytochemistry 71: 1474–1484.

Marinova, D. and F. Ribarova. 2007. HPLC determination of carotenoids in Bulgarian berries. J. Food Compos. Anal. 20: 370–374.

McGuire, R.G. 1992. Reporting of objective color measurements. HortScience 27: 1254–1255.

Nyman, N.A. and J.T. Kumpulainen. 2001. Determination of anthocyanidins in berries and red wine by high-performance liquid chromatography. J. Agric. Food Chem. 49: 4183–4187.

Oliveira, C., L.F. Amaro, O. Pinho, and I.M.P.L.V.O. Ferreira. 2010. Cooked blueberries: anthocyanin and anthocyanidin degradation and their radical-scavenging activity. J. Agric. Food Chem. 58: 9006–9012.

Prior, R.L., S.A. Lazarus, G. Cao, H. Muccitelli, and J.F. Hammerstone. 2001. Identification of procyanidins and anthocyanins in blueberries and cranberries (*Vaccinium* spp.) using high-performance liquid chromatography/mass spectrometry. J. Agric. Food Chem. 49: 1270–1276.

Ramazzotti, S., I. Filippetti, and C. Intrieri. 2008. Expression of genes associated with anthocyanin synthesis in red-purplish, pink, pinkish-green, and green grape berries from mutated 'Sangiovese' biotypes: a case study. Vitis 47: 147–151.

Ribera, A.E., M. Reyes-Diaz, M. Alberdi, G.E. Zuniga, and M.L. Mora. 2010. Antioxidant compounds in skin and pulp of fruits change among genotypes and maturity stages in highbush blueberry (*Vaccinium corymbosum* L.) grown in southern Chile. J. Soil Sci. Plant Nutr. 10: 509–536.

Rowan, D.D., M. Cao, K. Lin-Wang, M. Cooney, D.J. Jensen, P.T. Austin, M.B. Hunt, C. Norling, R.P. Hellens, R.J. Schaffer, and A.C. Allan. 2009. Environmental regulation of leaf color in red 35S:PAP1 *Arabidopsis thaliana*. New Phytol. 182: 102–115.

Veitch, N.C. and R.J. Grayer. 2011. Flavonoids and their glycosides, including anthocyanins. Nat. Prod. Rep. 28: 1626–1695.

Wang, S.Y., C.T. Chen, W. Sciarappa, C.Y. Wang, and M.J. Camp. 2008. Fruit quality, antioxidant capacity, and flavonoid content of organically and conventionally grown blueberries. J. Agric. Food Chem. 56: 5788–5794.

Wu, X. and R.L. Prior. 2005. Systematic identification and characterization of anthocyanins by HPLC-ESI-MS/MS in common foods in the United States: fruits and berries. J. Agric. Food Chem. 53: 2589–2599.

Xie, Q., Z. Hu, Y. Zhang, S. Tian, Z. Wang, Z. Zhao, Y. Yang, and G. Chen. 2014. Accumulation and molecular regulation of anthocyanin in purple tumorous stem

mustard (*Brassica juncea* var. *tumida* Tsen et Lee). J. Agric. Food Chem. 62: 7813−7821.

Yang, M., S.I. Koo, W.O. Song, and O.K. Chun. 2011. Food matrix affecting anthocyanin bioavailability: review. Curr. Med. Chem. 18: 291−300.

Zhang, Y., E. Butelli, and C. Martin. 2014. Engineering anthocyanin biosynthesis in plants. Curr. Opin. Plant Biol. 19: 81−90.

Zifkin, M., A. Jin, J.A. Ozga, L.I. Zaharia, J.P. Schernthaner, A. Gesell, S.R. Abrams, J.A. Kennedy, and C.P. Constabel. 2012. Gene expression and metabolite profiling of developing highbush blueberry fruit indicates transcriptional regulation of flavonoid metabolism and activation of abscisic acid metabolism. Plant Physiol. 158: 200−224.

CHAPTER II

Transcriptional Regulation of Abscisic Acid Biosynthesis and Signal Transduction, and Anthocyanin Biosynthesis in 'Bluecrop' Highbush Blueberry Fruit during Ripening

ABSTRACT

Blueberry fruit accumulate high levels of anthocyanins during ripening, which might be controlled by abscisic acid (ABA), a signal molecule in non-climacteric fruits. For an integrated view of the ripening process from ABA to anthocyanin biosynthesis, transcriptomes of 'Bluecrop' highbush blueberry fruit were analyzed using RNA-Seq at three ripening stages, categorized based on fruit skin coloration: pale green at ca. 30 days after full bloom (DAFB), reddish purple at ca. 40 DAFB, and dark purple at ca. 50 DAFB. Mapping the trimmed reads against the reference sequences yielded 25,766 transcripts. Of these, 143 transcripts were annotated to encode five ABA biosynthesis enzymes, four ABA signal transduction regulators, four ABA-responsive transcription factors, and 12 anthocyanin biosynthesis enzymes. The analysis of differentially expressed genes between the ripening stages revealed that 11 transcripts, including those encoding nine-*cis*-epoxycarotenoid dioxygenase, SQUAMOSA-class MADS box transcription factor, and flavonoid 3',5'-hydroxylase, were significantly up-regulated throughout the entire ripening stages. In fruit treated with 1 g L^{-1} ABA, at least nine transcripts of these 11 transcripts as well as one transcript encoding flavonoid 3'-hydroxylase were up-regulated, presumably promoting anthocyanin accumulation and fruit skin

coloration. These results will provide fundamental information demonstrating that ABA biosynthesis and signal transduction, and anthocyanin biosynthesis are closely associated with anthocyanin accumulation and skin coloration in highbush blueberry fruit during ripening.

Key words: abscisic acid, anthocyanins, highbush blueberry, fruit coloration, non-climacteric fruits, transcriptome analysis, *Vaccinium corymbosum*

INTRODUCTION

Climacteric fruits such as apple, banana, and tomato, generate a burst of ethylene at the onset of ripening (Giovannoni et al., 2001; Kondo et al., 2009; Xu et al., 2012). The burst of ethylene accelerates ripening of climacteric fruits. These changes act as a signal of the initiation of ripening in all climacteric fruits. Ripening of climacteric fruits is also stimulated by exogenous ethylene. In contrast, non-climacteric fruits, including strawberry, grape, and blueberry, do not show a dramatic change in ethylene content, and are not affected by exogenous ethylene (Chai et al., 2011; Frenkel, 1972; Symons et al., 2012), although some such fruits have ethylene receptors (Chen et al., 2016). However, ripening of non-climacteric fruits in association with hormonal regulation remains poorly understood.

Evidence that the ripening of non-climacteric fruits is associated with abscisic acid (ABA) has been accumulated. Fruit coloration during ripening is promoted by ABA application in many non-climacteric fruits, including blueberry (Oh et al., 2018), grape (Koyama et al., 2010; Villalobos-González et al., 2016; Wheeler et al., 2009), strawberry (Chai et al., 2011; Jia et al., 2011), and sweet cherry (Luo et al., 2014; Shen et al., 2014). Genes involved in ABA biosynthesis and signal transduction have been reported to be regulated during ripening as those in anthocyanin biosynthesis and furthermore their regulations were enhanced by ABA application. For example, *β-carotene 3-hydroxylase* (*BCH*) (Ampomah-Dwamena et al., 2009) and *nine-cis-epoxycarotenoid dioxygenases* (*NCED*s) (Wheeler et al., 2009; Zifkin et al., 2012) involved in ABA biosynthesis and *pyrabactin resistance/pyrabactin resistance-like/regulatory components of ABA receptors* (*PYR*/*PYL/RCAR*) involved in ABA signal transduction were up-regulated during

ripening. Conversely, silencing *NCED*s resulted in colorless phenotypes in strawberry (Jia et al., 2011), sweet cherry (Shen et al., 2014), and bilberry fruits (Karppinen et al., 2018). The *PYR*-silenced strawberry fruit did not undergo skin coloration regardless of ABA application (Chai et al., 2011). These findings suggest that ABA biosynthesis and signal transduction are closely associated with anthocyanin biosynthesis during ripening.

Blueberry fruit accumulate high level of anthocyanins during ripening, leading to a highly noticeable coloration (Oh et al., 2018; Zifkin et al., 2012). The coloration with anthocyanin accumulation makes blueberry fruit suitable for studies of ripening. As the blueberry fruit undergo ripening, their skin color changes from pale green to dark blue or purple according to the accumulations of the individual anthocyanins derived from a particular anthocyanidin type (Chung et al., 2016; Oh et al., 2018; Wu et al., 2005; Zifkin et al., 2012). Correlation of fruit skin coloration and anthocyanin accumulation during ripening has often been demonstrated in blueberry fruit (Chung et al., 2016; Oh et al., 2018).

Transcriptome analysis using RNA-Seq has widely been applied to explain various cellular metabolisms (Cao et al., 2017; Ozsolak et al., 2011; Wang et al., 2009). Although transcripts encoding the enzymes involved in anthocyanin biosynthesis have been sequenced in blueberry fruit (Gupta et al., 2015; Li et al., 2012; Li et al., 2016; Lin et al., 2018; Zifkin et al., 2012), the transcript expressions regarding ABA and anthocyanin biosynthesis have not been investigated for explaining fruit coloration during ripening.

In this study, the transcriptomes of ‘Bluecrop’ highbush blueberry (*Vaccinium corymbosum*) fruit were analyzed using RNA-Seq to obtain an integrated view of the ripening process from ABA to anthocyanin biosynthesis. Effects of exogenous ABA on

anthocyanin accumulation and its regulatory transcript expression were also characterized.

MATERIALS AND METHODS

Plant materials

Ten-year-old ‘Bluecrop' highbush blueberry shrubs were grown in the experimental orchard of Seoul National University, Suwon (37° 17’ N, 127° 00’ E), Republic of Korea. Fruit were categorized into three ripening stages based on their skin coloration: (1) pale green at ca. 30 days after full bloom (DAFB), (2) reddish purple at ca. 40 DAFB, and (3) dark purple at ca. 50 DAFB (Fig. II-1). Ninety fruit at each stage were harvested from three shrubs during ripening to provide three replicates with 30 fruit each in the sampling design. All harvested fruit were immediately frozen in liquid nitrogen and stored at –80°C until use for the transcriptome analysis.

ABA treatments

Fruit clusters attached to the shrubs were dipped into a solution containing 1 g L^{-1} (±) ABA (Sigma-Aldrich, St. Louis, MO, USA) for 1 min at pale green stage, according to the methods of Jeong et al. (2004). The ABA concentration was chosen based on the results of our previous study (Oh et al., 2018), and the ABA solution was prepared with 5% ethanol containing 0.1% (v/v) Tween 80. All treatments were conducted after sunset to avoid the photodegradation of ABA (Zaharia et al., 2005). Control fruit were treated with 5% ethanol containing 0.1% Tween 80 without ABA. These experiments were employed in a randomized complete block design with three replications consisting of five shrubs each. Fifty fruit were randomly sampled from each replication block at 5 days after treatment (DAT) when the fruit skin color began to change. All harvested fruit were immediately frozen in liquid nitrogen

Fig. II-1. Calyx end (top) and stem end (bottom) of ‘Bluecrop’ highbush blueberry fruit during ripening. Three ripening stages are based on skin coloration: pale green at ca. 30 days after full bloom (DAFB), reddish purple at ca. 40 DAFB, and dark purple at ca. 50 DAFB. Bar = 1 cm.

and stored at –80°C until use for the quantification of individual anthocyanins and the expression profiling of their related transcripts.

Determination of fruit color

Fruit skin colors were measured using a spectrophotometer (CM-2500d; Minolta Co., Osaka, Japan) and described by the CIE L*, a*, and b* color space coordinates (McGuire, 1992). The L* value represents the lightness of colors, with a range of 0 to 100 (0, black; 100, white). The a* value is negative for green and positive for red. The b* value is negative for blue and positive for yellow. For each fruit, the values were measured at three different points along the fruit equator.

Determination of individual anthocyanin contents

Anthocyanins in whole fruit were extracted according to the method described by Gavrilova et al. (2011), with some modifications. Approximately 5 g of ground fruit tissues was added to 10 mL of a solution containing acetone:acetic acid (99:1, v/v). The homogenate was sonicated for 15 min and centrifuged at 1,900 × *g* for 15 min. The supernatants were evaporated until dry using a rotary evaporator (Eyela N-1000S-W; Tokyo Rikakikai Co., Tokyo, Japan) at 37°C, then completely redissolved in 10 mL of 20% methanol and filtered through a PTFE filter with a pore size of 0.45 μm (Whatman Inc., Florham Park, NJ, USA).

Individual anthocyanin contents were determined using a high performance liquid chromatography (HPLC)-diode array detector system (Dionex Ultimate 3000; Thermo Fisher Scientific, Waltham, MA, USA) equipped with a VDSpher PUR C-18 column (4.6 × 150 mm, 3.5 μm; VDS Optilab, Berlin, Germany). Anthocyanins were eluted using a gradient of mobile phase A (aqueous 5% [v/v] formic acid) and

mobile phase B (5% [v/v] formic acid in acetonitrile) in the following sequence: 0-30 min, 5-45% B; 30-35 min, 45% B; 35-36 min, 45-5% B; and 36-40 min, 5% B. The flow rate was 0.8 mL min^{-1}, and detections were made at 520 nm. Cyanidin, delphinidin, peonidin, and petunidin 3-*O*-glucosides (Sigma-Aldrich), and malvidin and pelargonidin 3-*O*-glucosides (Polyphenols AS, Sandnes, Norway) were used as standards.

RNA extraction

Total RNA was extracted from whole fruit at each stage as described by Jaakola et al. (2001), with slight modifications. Extraction buffer (2% hexadecyltrimethylammonium bromide, 2% polyvinylpyrrolidone, 100 mM Tris-HCl [pH 8.0], 25 mM EDTA [pH 8.0], 2.0 M NaCl, and 2% β-mercaptoethanol) was heated to 65°C and then 900 μL of the extraction buffer was transferred to a 2-mL microfuge tube containing 100 mg of powdered fruit tissues and incubated at 65°C for 10 min. An equal volume of chloroform:isoamyl alcohol (24:1, v/v) was added, vortexed for 5 s, and centrifuged at 10,000 × *g* at 4ºC for 10 min. The supernatant of 750 μL was recovered and mixed with an equal volume of the chloroform:isoamyl alcohol. Following the centrifugation as above, the supernatant of 600 μL was transferred to a new 2-mL tube, and an equal volume of 6 M LiCl solution was added. The mixture was incubated on ice for 30 min and centrifuged at 21,000 × g at 4°C for 20 min to precipitate the RNA. The pellet was resuspended in 500 μL of preheated (65°C) SSTE buffer (0.5% sodium lauryl sulfate, 1 M NaCl, 1 M Tris-HCl [pH 8.0], and 10 mM EDTA [pH 8.0]) while gentle shaking. An equal volume of the chloroform:isoamyl alcohol was added, and the mixture was centrifuged at 21,000 × g at 4°C for 10 min, then dried and resuspended in 20 μL

diethyl pyrocarbonate-treated water. Finally, the solution was heated at 65°C for 5 min to completely dissolve the RNA. The quality of the extracted RNA samples was assessed using a NanoDrop ND1000 (Thermo Fisher Scientific), following the confirmation of the RNA integrity using an Agilent 2100 Bioanalyzer (Agilent Technologies, Waldbronn, Germany).

RNA-Seq and sequence processing

Nine cDNA libraries were constructed for whole fruit at pale green, reddish purple, and dark purple stages from three replicates with 30 each, using a TruSeq small RNA library preparation kit (Illumina, San Diego, CA, USA), and sequenced using an Illumina HiSeq 2000 system. The quality of the data produced was confirmed using the R package fastqcr (version 0.1.2). Adapters and low-quality reads, including short reads (< 36 bp) and reads with a Phred score Q ≤ 20, were removed from the raw data using the R package QuasR (version 1.22.1). The trimmed reads were mapped to the reference highbush blueberry transcriptome (*V. corymbosum* RefTrans V1) from the Genome Database for *Vaccinium* using Cufflinks (version 2.2.1). The RNA-Seq data were deposited to the National Center for Biotechnology Information (NCBI) (accession No. PRJNA533973).

Gene ontology (GO) annotation and identification of differentially expressed genes (DEGs)

GO assignments were made to the mapped reads using InterProScan at the European Bioinformatics Institute through Blast2GO. The obtained GO terms were classified and plotted using WEGO (version 2.0).

To identify the DEGs, the mapped transcripts were functionally annotated using

the KEGG database, and the expression levels of the transcripts were calculated as fragments per kilobase of transcript per million mapped reads (FPKM) using Cuffdiff (version 2.2.1). The FPKM values were normalized, and statistical analyses were performed on the fold change values using a Student′s *t*-test at $P < 0.05$. The clustered DEGs based on their $\log_2$ FPKM values were plotted using the R package pheatmap (version 1.0.12). The DEGs were identified from three replications at each ripening stage.

Quantitative polymerase chain reaction (qPCR) analysis

Primer sets were designed using the NCBI PrimerBLAST. Sequences of the forward and reverse primers used for the qPCR are listed in Table II-1. The relative expression levels of the transcripts were determined using a Rotor-Gene Q (Qiagen, Valencia, CA, USA) and a Rotor-Gene SYBR® Green PCR kit (Qiagen). The results were standardized to the expression level of the gene encoding glyceraldehyde 3-phosphate dehydrogenase, as described by Zifkin et al. (2012). The relative expression levels were plotted using the Prism program (version 8.0.2; GraphPad Software Inc., San Diego, CA, USA).

Statistical analysis

Statistically significant differences among means were determined by Student's *t*-test at $P < 0.05$ using the R 3.2.2 software package (http://www.r-project.org).

Table II-1. Sequences of primers used for quantitative polymerase chain reaction.

Transcript ID	Primer sequence
XLOC_002223	F: GTGGAAATACCGTTGGATGG
	R: CTCCCAAGCATTCCACAAGT
XLOC_020802	F: CCCTCTCAGCCAGTGTCTTC
	R: CACCTTGACCCTGAGAGAGC
XLOC_011961	F: GCGTGTGTGCTGTTCATTTT
	R: CCATTCAAGTGCACAAGCTG
XLOC_013012	F: GGGTGACTGGGTGAAAAGAA
	R: CCTTTAACGGGCAAGCAATA
XLOC_024963	F: TCAACTTGGCCTTCTCCAGT
	R: ACCCGAGGCAACAGTGTATC
XLOC_006400	F: CAGTTTTTGAAGACGCACGA
	R: TCCAAGGCCTTAGCAGAGAA
XLOC_025538	F: GAGTCGGAGTTGGGTCACAT
	R: TCGCCCACGTTAAATAGTCC
XLOC_001004	F: ACCCTTCCACCCCACTTAAC
	R: CGGAATCAACTCGAAATCGT
XLOC_025532	F: TGGGATTGGAAGAAGACAGG
	R: GATCCATTTGCCCTCGTAGA
XLOC_001255	F: ATGCTCTCTGTCGGCTCATT
	R: TTGCTTTGTGCAGAACTTGG
XLOC_008271	F: AGCCCAGTTTCCGGTACTCT
	R: TCCTCTGTTCAACCGATTCC

F, forward; R, reverse.

RESULTS AND DISCUSSION

Fruit skin coloration and anthocyanin accumulation during ripening

The skin color of the 'Bluecrop' highbush blueberry fruit changed during ripening (Fig. II-1). With the calyx turning green to purple, the exocarp was mostly tinted red at reddish purple stage and then shifted bluer at dark purple stage (Fig. II-1). The reddish purple and dark purple stages indicated fruit at turning point and fully ripe stages, respectively (Chea et al., 2019). Our previous study revealed that the skin coloration of 'Bluecrop' highbush blueberry fruit during ripening correlated with the accumulation of anthocyanins, especially of delphinidin and delphinidin derivatives (Chung et al., 2016).

ABA as a positive regulator of anthocyanin accumulation during ripening

In the ABA-treated fruit, the calyx turned dark purple and the exocarp changed to red or purple at 5 DAT, but untreated fruit remained green (Fig. II-2). Although the L* value of the ABA-treated fruit was not significantly different from that of untreated fruit, the a* and b* values of the ABA-treated fruit were significantly higher and lower, respectively, than those of untreated fruit (Table II-2). These results indicated that the ABA-treated fruit were redder and bluer than untreated fruit. Accelerated skin coloration by ABA application has also been reported in other non-climacteric fruits, including strawberry (Jia et al., 2011; Li et al., 2014), grape (Jeong et al., 2004; Karppinen et al., 2018; Koyama et al., 2010), and sweet cherry (Shen et al., 2014).

The ABA application also accelerated the accumulation of individual anthocyanins in 'Bluecrop' highbush blueberry fruit (Table II-3). At 5 DAT, no

Fig. II-2. Calyx end (top) and stem end (bottom) of 'Bluecrop' highbush blueberry fruit at 5 days after treatment with or without 1 g L^{-1} (±) ABA at pale green stage (ca. 30 days after full bloom). Bar = 1 cm.

Table II-2. Chromaticity values of 'Bluecrop' highbush blueberry fruit at 5 days after the treatment with or without 1 g L^{-1} (±) ABA at pale green stage (ca. 30 days after full bloom).

Treatment	L*	a*	b*
Untreated	75.7 a[1]	−15.1 b	25.1 a
ABA-treated	60.7 a	20.2 a	15.3 b

[1]Means within columns followed by different letters are significantly different according to Student's *t*-test at $P < 0.05$.

Table II-3. Individual anthocyanin contents in 'Bluecrop' highbush blueberry fruit at 5 days after the treatment with or without 1 g L^{-1} (±) ABA at pale green stage (ca. 30 days after full bloom).

Treatment	Cya-glu	Del-glu	Mal-glu	Pel-glu	Peo-glu	Pet-glu
	($\mu g\ g^{-1}$ FW)					
Untreated	nd[1]	nd	nd	nd	nd	nd
ABA-treated	80 ± 14.1[2]	11 ± 3.4	35 ± 4.4	nd	nd	2 ± 0.9

Cya-glu, cyanidin 3-*O*-glucoside; Del-glu, delphinidin 3-*O*-glucoside; Mal-glu, malvidin 3-*O*-glucoside; Pel-glu, pelargonidin 3-*O*-glucoside; Peo-glu, peonidin 3-*O*-glucoside; Pet-glu, petunidin 3-*O*-glucoside.

[1]Not detected.

[2]Means with standard errors from three replications with 30 fruit each.

anthocyanins were detected in untreated fruit, while the ABA-treated fruit accumulated four anthocyanins; cyanidin, malvidin, delphinidin, and petunidin 3-*O*-glucosides (Table II-2). However, neither pelargonidin nor peonidin 3-*O*-glucosides were found in the ABA-treated fruit (Table II-2). According to our previous study in 'Bluecrop' highbush blueberry fruit (Chung et al., 2016), cyanidins, malvidins, and delphinidins began to accumulate from reddish purple stage and petunidins were accumulated at dark purple stage, but no pelargonidins were accumulated throughout the entire ripening stages. No pelargonidin accumulation was also observed in 'Jersey' highbush blueberry fruit regardless of ABA application (Oh et al., 2018). The absence of pelargonidin is a common characteristic of the fruits of the Ericaceae (Jaakola et al., 2002; Ribera et al., 2010). The ABA application promoted the accumulation of anthocyanins, especially of delphinidin derivatives, with a temporary increase in ABA content and thus accelerated fruit skin coloration (Oh et al., 2018).

Transcriptome and GO analyses

As the results of RNA-Seq in 'Bluecrop' highbush blueberry fruit during ripening, the trimmed reads ranged from 25,552,078 to 28,546,644 with Q30 of 94.9 to 98.2% and GC content of 48.0 to 48.9% (Table II-4). The total bases of average 2.58 to 2.88 $\times 10^9$ were obtained (Table II-4).

Of the 25,766 assembled transcripts, 10,998 transcripts were assigned and classified into 44 groups within the three GO categories: cellular component, molecular function, and biological process (Fig. II-3). The majority of the GO terms (51.7%) were assigned to molecular function, while 34.3% and 14.0% were assigned to biological process and cellular component, respectively (Fig. II-3).

Table II-4. RNA-Seq results of 'Bluecrop' highbush blueberry fruit during ripening.

Ripening stage[1]	No. of total reads	No. of total bases	Q30 (%)	GC content (%)
Pale green	28,546,644	2,883,211,044	95.3	48.9
Reddish purple	25,552,078	2,580,878,759	94.9	48.6
Dark purple	27,439,060	2,771,345,060	98.2	48.0

Average read length is 101 bp, and each value is the mean from three replications with 30 fruit each.

[1]Three ripening stages based on skin coloration: pale green at ca. 30 days after full bloom (DAFB), reddish purple at ca. 40 DAFB, and dark purple at ca. 50 DAFB.

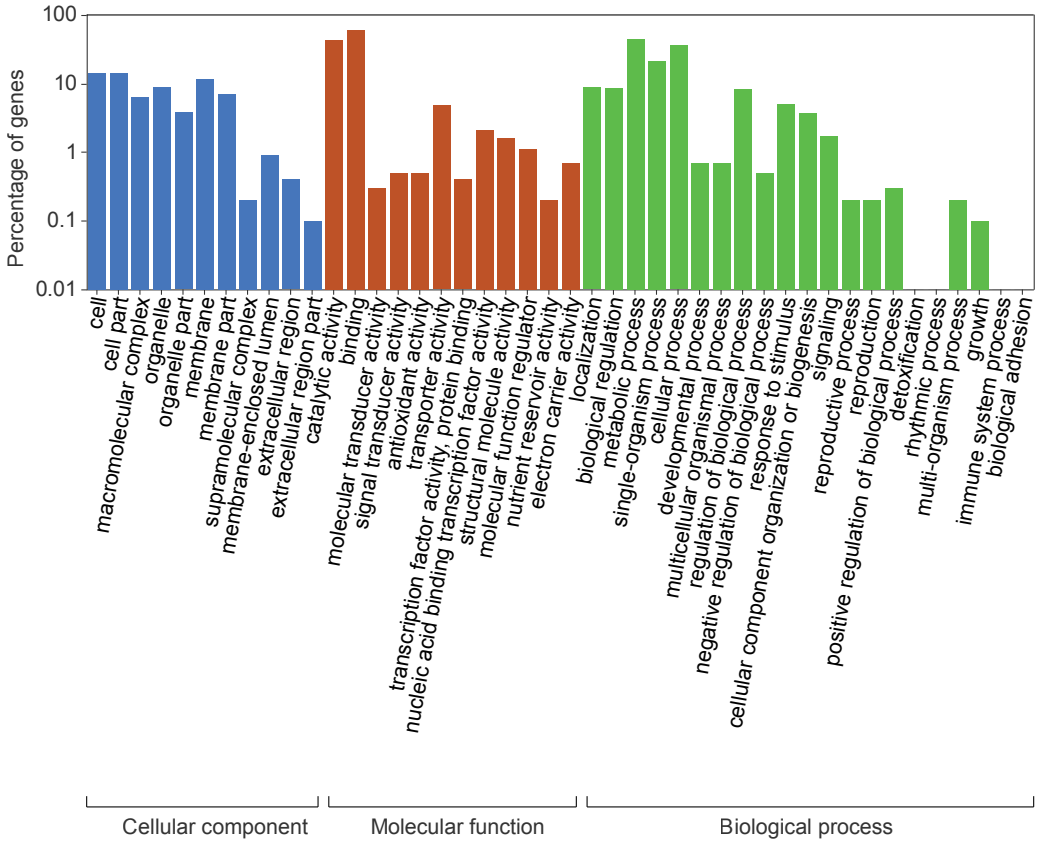

Fig. II-3. Functional annotation of the transcripts of 'Bluecrop' highbush blueberry fruit based on gene ontology categorization. The y-axis indicates the percentage of genes, expressed as a $\log_{10}$ scale.

Transcripts associated with binding and catalytic activity were typical in molecular function, while those associated with cell and cell part were highly represented in cellular component. For biological process, metabolic process and cellular process were the most highly represented groups. These two dominant groups in each GO category for 'Bluecrop' highbush blueberry fruit (Fig. II-3) have also been observed in the same cultivar (Rowland et al., 2012) and in other cultivars of 'Northland' (Li et al., 2012) and 'O'Neal' (Gupta et al., 2015).

Functional annotation of the transcripts involved in ABA biosynthesis and their DEG analysis

An intermediate of terpenoid pathway, β-carotene, is sequentially converted to form ABA by the actions of enzymes, such as BCH, zeaxanthin epoxidase (ZEP), NCED, xanthoxin dehydrogenase (ABA2), and abscisic-aldehyde oxidase (AAO3) (Fig. II-4) (Nambara and Marion-Poll, 2005).

In the present study, 44 transcripts were annotated to encode five enzymes involved in ABA biosynthesis: five *BCH*s, six *ZEP*s, eight *NCED*s, four *ABA2*s, and one *AAO3* (Fig. II-5). The expressions of one *BCH* (XLOC_014503), six *NCED*s (XLOC_002223, XLOC_003903, XLOC_016360, XLOC_016358, XLOC_021727, and XLOC_024952), and one *AAO3* (XLOC_023979) were significantly up- or down-regulated during ripening, while the others were not significantly regulated (Table II-5).

The *BCH* was significantly up-regulated from pale green to reddish purple stages (Table II-5), as observed in kiwifruit (Ampomah-Dwamena et al., 2009). However, ABA accumulation was significantly reduced in two allelic *dsm2* mutants of rice, which lacked a functional BCH protein (Du et al., 2010). NCEDs and their isoforms

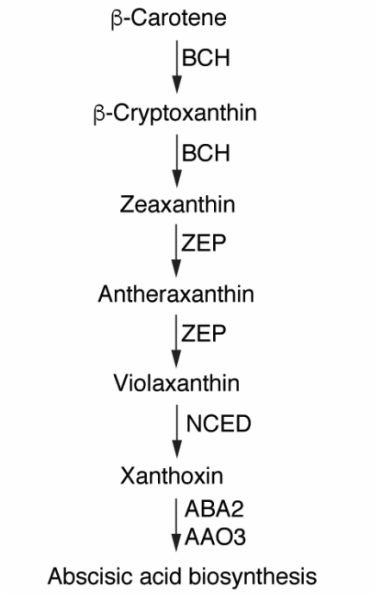

Fig. II-4. Schematic view of the ABA biosynthesis pathway (modified from Nambara and Marion-Poll [2005]). BCH, β-carotene 3-hydoroxylase; ZEP, zeaxanthin epoxidase; NCED, nine-*cis*-epoxycarotenoid dioxygenase; ABA2, xanthoxin dehydrogenase; AAO3, abscisic-aldehyde oxidase.

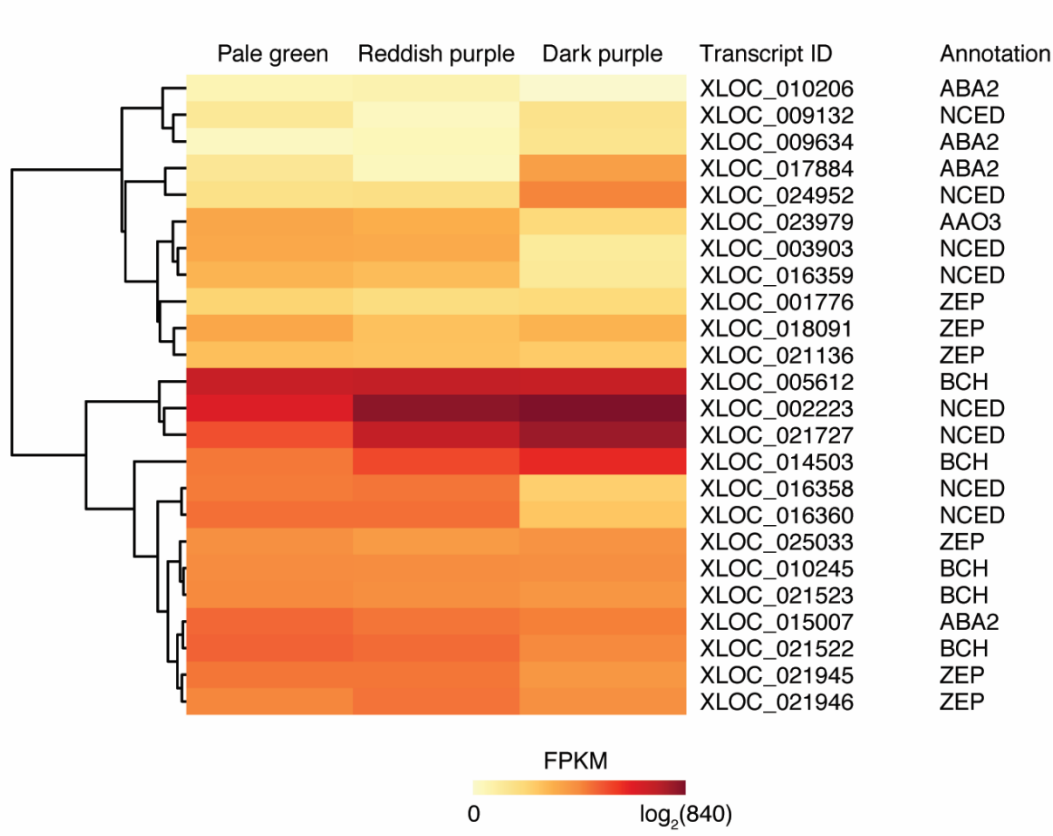

Fig. II-5. Heatmap of the $\log_2$ FPKM expression of candidate transcripts involved in ABA biosynthesis in 'Bluecrop' highbush blueberry fruit during ripening. Three ripening stages are based on fruit skin coloration: pale green at ca. 30 days after full bloom (DAFB), reddish purple at ca. 40 DAFB, and dark purple at ca. 50 DAFB. The differentially expressed genes were clustered based on their FPKM values. BCH, β-carotene 3-hydoroxylase; ZEP, zeaxanthin epoxidase; NCED, nine-*cis*-epoxycarotenoid dioxygenase; ABA2, xanthoxin dehydrogenase; AAO3, abscisic-aldehyde oxidase.

Table II-5. Fold changes (FC) in the transcriptional expression involved in abscisic acid biosynthesis in 'Bluecrop' highbush blueberry fruit during ripening.

		Pale green to reddish purple		Reddish purple to dark purple	
Annotation	Transcript ID	$\log_2$ FC	*P* value	$\log_2$ FC	*P* value
BCH	XLOC_005612	−0.18	0.80^{ns}	−0.62	0.21^{ns}
	XLOC_010245	−0.13	0.86^{ns}	−0.29	0.63^{ns}
	XLOC_014503	−0.02	0.98^{ns}	−0.09	0.92^{ns}
	XLOC_021522	0.10	0.89^{ns}	−0.10	0.89^{ns}
	XLOC_021523	1.03	0.01**	0.74	0.06^{ns}
ZEP	XLOC_001776	−0.89	0.11^{ns}	0.45	0.53^{ns}
	XLOC_018091	−0.48	0.63^{ns}	0.16	0.91^{ns}
	XLOC_021136	−0.38	0.47^{ns}	0.25	0.67^{ns}
	XLOC_021945	−0.07	0.96^{ns}	−0.34	0.74^{ns}
	XLOC_021946	0.01	0.99^{ns}	−0.81	0.12^{ns}
	XLOC_025033	0.37	0.48^{ns}	−0.63	0.19^{ns}
NCED	XLOC_002223	−2.60	1.00^{ns}	3.15	0.12^{ns}
	XLOC_003903	−0.23	0.86^{ns}	−2.47	0.15^{ns}
	XLOC_009132	−0.08	0.92^{ns}	−3.25	0.00***
	XLOC_016358	0.03	0.97^{ns}	−2.60	0.00***
	XLOC_016359	0.11	0.90^{ns}	−2.82	0.00***
	XLOC_016360	0.13	0.91^{ns}	3.44	0.00***
	XLOC_021727	2.01	0.00***	0.25	0.82^{ns}
	XLOC_024952	2.23	0.00***	0.84	0.10^{ns}
ABA2	XLOC_009634	−2.56	1.00^{ns}	5.82	0.10^{ns}
	XLOC_010206	−0.29	0.59^{ns}	−0.22	0.72^{ns}

Table II-5. Continued.

		Pale green to reddish purple		Reddish purple to dark purple	
Annotation	Transcript ID	$\log_2$ FC	*P* value	$\log_2$ FC	*P* value
	XLOC_015007	0.38	1.00^{ns}	0.07	0.95^{ns}
	XLOC_017884	0.76	1.00^{ns}	2.44	1.00^{ns}
AAO3	XLOC_023979	−0.28	0.60^{ns}	−1.64	0.00^{***}

^{ns,*,**,***} Non-significant or significant at $P < 0.05$, 0.01, or 0.001, respectively.

BCH, β-carotene 3-hydoroxylase; ZEP, zeaxanthin epoxidase; NCED, nine-*cis*-epoxycarotenoid dioxygenase; ABA2, xanthoxin dehydrogenase; AAO3, abscisic-aldehyde oxidase.

have been identified in many plant species, including bilberry (Jaakola et al., 2010; Karppinen et al., 2013, 2018), tomato (Sun et al., 2012; Zhang et al., 2009), and grape (Lund et al., 2008; Pilati et al., 2017; Young et al., 2012). These enzymes were differentially expressed depending on tissues, developmental stages, and environmental conditions (Chernys and Zeevart, 2000). *NCED* expression was reported to temporarily increase with the increased ABA contents during ripening of grape (Wheeler et al., 2009) and 'Rubel' highbush blueberry fruit (Zifkin et al., 2012). Of the six *NCED*s, two *NCED*s (XLOC_002223 and XLOC_021727) were also significantly up-regulated from pale green to reddish purple stages (Table II-5). From reddish purple to dark purple stages, one *NCED* (XLOC_024952) was up-regulated, while the remaining three *NCED*s were down-regulated (Table II-5). The *AAO3* was significantly down-regulated from reddish purple to dark purple stages, but its FPKM values remained low throughout the entire ripening stages (Fig. II-5). Since the transcripts involved in ABA biosynthesis were differentially expressed during ripening (Fig. II-5, Table II-5), ABA might trigger the signal transduction for biosynthesizing anthocyanins responsible for characteristic coloration in highbush blueberry fruit.

Functional annotation of the transcripts involved in ABA signal transduction and their DEG analysis

In ABA signal transduction (Fig. II-6), ABA activates PYR/PYL/RCAR (Pilati et al., 2017), and then the ABA-activated PYR/PYL/RCAR inhibits a protein phosphatase 2C (PP2C) (Park et al., 2009), leading to the activation of sucrose non-fermenting-1 -related protein kinase 2 (SnRK2). The SnRK2 regulates ABA-responsive element binding factor (ABF) (Li et al., 2011; Pilati et al., 2017).

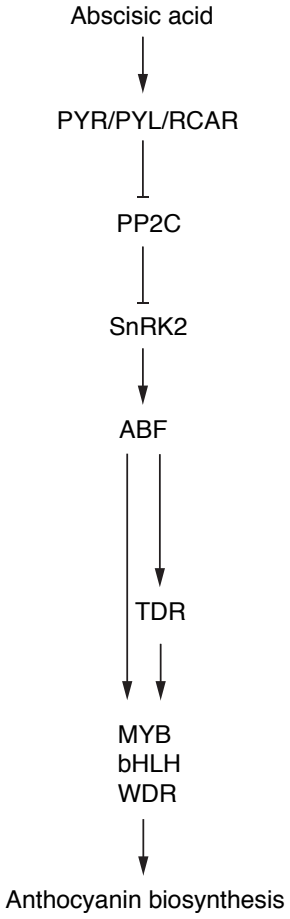

Fig. II-6. Schematic view of the ABA signal transduction pathway (modified from Li et al. [2011]). PYR/PYL/RCAR, pyrabactin resistance/pyrabactin resistance-like/regulatory components of ABA receptors; PP2C, protein phosphatases type 2C; SnRK2, sucrose non-fermenting-1-related protein kinase 2; ABF, ABA-responsive element binding factor; TDR, SQUAMOSA-class MADS box transcription factor; MYB, myeloblastosis transcription factor; bHLH, basic helix-loop-helix transcription factor; WDR, β-transduction repeat transcription factor.

In the present study, 46 transcripts were annotated to encode four signal transduction regulators (nine *PYL*s, ten *PP2C*s, 12 *SnRK2*s, and 15 *ABF*s) (Fig. II-7). Of the signal transduction regulators, one *PYL* (XLOC_025240) was significantly up-regulated throughout the entire ripening stages, while 14 transcripts (five *PYL*s [XLOC_001385, XLOC_006253, XLOC_014772, XLOC_ 018382, and XLOC_019042], four *PP2C*s [XLOC_002375, XLOC_008259, XLOC_014109, and XLOC_0195742], two *SnRK2*s [XLOC_003694 and XLOC_008135], and three *ABF*s [XLOC_0160006, XLOC_021956, and XLOC_023170]) were significantly up-regulated from reddish purple to dark purple stages (Table II-6). However, one *SnRK2* (XLOC_022345) and one *ABF* (XLOC_009041) were down-regulated throughout the entire ripening stages, but the others were not significantly regulated (Table II-6).

In *Arabidopsis*, ABA application induced the transcriptional expression of the PYR/PYL/RCAR family (Yang et al., 2017). In strawberry fruit, similarly, ABA application enhanced the up-regulation of a *PYR* among the family during ripening, while no coloration occurred in the *PYR*-silenced fruit regardless of ABA application (Chai et al., 2011). However, up-regulation of the four *PP2C*s and down-regulation of the one *SnRK2* and one *ABF* in the present study (Table II-6) were contradictory to the results in *Arabidopsis* (Yang et al., 2017). The question of if there is ABA signal transduction process specific for highbush blueberry fruit remains to be answered unequivocally.

ABF in ABA signal transduction (Fig. II-6) regulates various transcription factors, such as SQUAMOSA-class MADS box (TDR), myeloblastosis (MYB), basic helix-loop-helix (bHLH), and β-transduction repeat (WDR), which are associated with the gene expressions in anthocyanin biosynthesis (Hu et al., 2019;

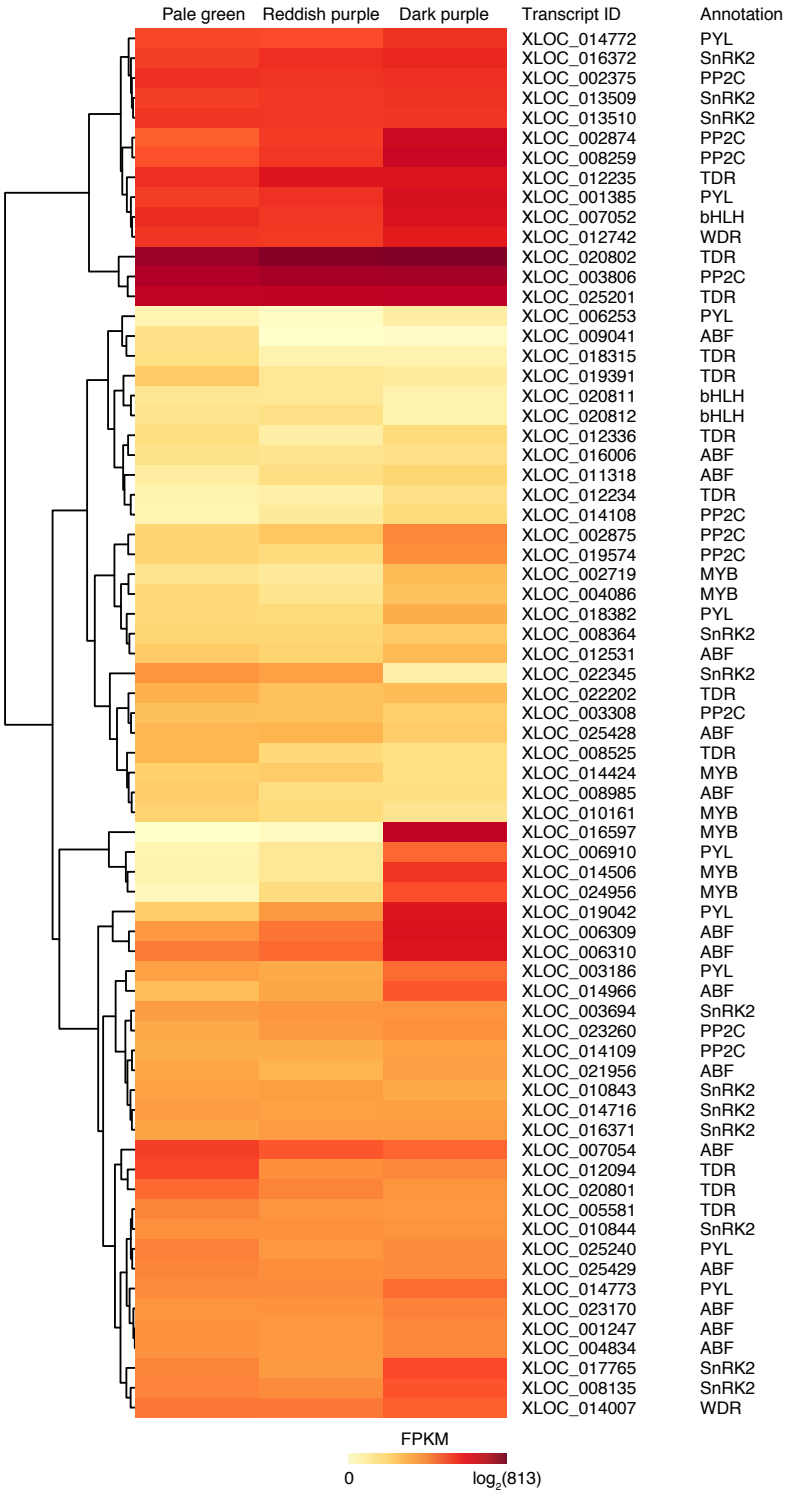
Pale green
Reddish purple
Dark purple
Transcript ID
Annotation
XLOC_014772 PYL
XLOC_016372 SnRK2
XLOC_002375 PP2C
XLOC_013509 SnRK2
XLOC_013510 SnRK2
XLOC_002874 PP2C
XLOC_008259 PP2C
XLOC_012235 TDR
XLOC_001385 PYL
XLOC_007052 bHLH
XLOC_012742 WDR
XLOC_020802 TDR
XLOC_003806 PP2C
XLOC_025201 TDR
XLOC_006253 PYL
XLOC_009041 ABF
XLOC_018315 TDR
XLOC_019391 TDR
XLOC_020811 bHLH
XLOC_020812 bHLH
XLOC_012336 TDR
XLOC_016006 ABF
XLOC_011318 ABF
XLOC_012234 TDR
XLOC_014108 PP2C
XLOC_002875 PP2C
XLOC_019574 PP2C
XLOC_002719 MYB
XLOC_004086 MYB
XLOC_018382 PYL
XLOC_008364 SnRK2
XLOC_012531 ABF
XLOC_022345 SnRK2
XLOC_022202 TDR
XLOC_003308 PP2C
XLOC_025428 ABF
XLOC_008525 TDR
XLOC_014424 MYB
XLOC_008985 ABF
XLOC_010161 MYB
XLOC_016597 MYB
XLOC_006910 PYL
XLOC_014506 MYB
XLOC_024956 MYB
XLOC_019042 PYL
XLOC_006309 ABF
XLOC_006310 ABF
XLOC_003186 PYL
XLOC_014966 ABF
XLOC_003694 SnRK2
XLOC_023260 PP2C
XLOC_014109 PP2C
XLOC_021956 ABF
XLOC_010843 SnRK2
XLOC_014716 SnRK2
XLOC_016371 SnRK2
XLOC_007054 ABF
XLOC_012094 TDR
XLOC_020801 TDR
XLOC_005581 TDR
XLOC_010844 SnRK2
XLOC_025240 PYL
XLOC_025429 ABF
XLOC_014773 PYL
XLOC_023170 ABF
XLOC_001247 ABF
XLOC_004834 ABF
XLOC_017765 SnRK2
XLOC_008135 SnRK2
XLOC_014007 WDR
FPKM
0
log2(813)

Fig. II-7. Heatmap of the $\log_2$ FPKM of candidate transcripts involved in ABA signal transduction in 'Bluecrop' highbush blueberry fruit during ripening. Three ripening stages are based on fruit skin coloration: pale green at ca. 30 days after full bloom (DAFB), reddish purple at ca. 40 DAFB, and dark purple at ca. 50 DAFB. The differentially expressed genes were clustered based on their FPKM values. PYR/PYL/RCAR, pyrabactin resistance/pyrabactin resistance-like/regulatory components of ABA receptors; PP2C, protein phosphatases type 2C; SnRK2, sucrose non-fermenting-1-related protein kinase 2; ABF, ABA-responsive element binding factor; TDR, SQUAMOSA-class MADS box transcription factor; MYB, myeloblastosis transcription factor; bHLH, basic helix-loop-helix transcription factor; WDR, β-transduction repeat transcription factor.

Jaakola et al., 2010; Karppinen et al., 2018).

In the present study, 21 transcripts were annotated to encode four ABA-responsive transcription factors (ten *TDR*s, seven *MYB*s, two *bHLH*s, and two *WDR*s) (Fig. II-7). Of the ABA-responsive transcription factors, *TDR* (XLOC_020802) was most highly expressed throughout the entire ripening stages (Fig. II-7). However, two *TDR*s (XLOC_008525 and XLOC_012094) were significantly down-regulated from pale green to reddish purple stages and their expressions remained low thereafter (Table II-6). Four *MYB*s (XLOC_002719, XLOC_004086, XLOC_014506, and XLOC_024956) and one *bHLH* (XLOC_007502) were significantly up-regulated from reddish purple to dark purple stages, but the others were not significantly regulated throughout the entire ripening stages (Table II-6).

In bilberry fruit, *TDR* and *MYB* were found to be sequentially up-regulated during ripening and the up-regulations were enhanced by ABA application, increasing the anthocyanin accumulation (Jaakola et al., 2010). ABA application also enhanced the expressions of *bHLH* as well as *MYB* in grape fruit (Rattanakon et al., 2016). Silencing *TDR* and *MYB* led to a decrease in anthocyanin accumulation and its associated gene expressions in sweet cherry (Shen et al., 2014) and bilberry fruits (Jaakola et al., 2010).

Functional annotation of the transcripts involved in anthocyanin biosynthesis and their DEG analysis

Anthocyanins are biosynthesized by the sequential actions of enzymes, such as chalcone synthase (CHS), chalcone isomerase (CHI), flavanone 3-hydroxylase (F3H), flavonoid 3’-hydroxylase (F3´H), flavonoid 3’,5’-hydroxylase (F3’5’H),

Table II-6. Fold changes (FC) in the transcriptional expression involved in abscisic acid signal transduction in 'Bluecrop' highbush blueberry fruit during ripening.

		Pale green to reddish purple		Reddish purple to dark purple	
Annotation	Transcript ID	$\log_2$ FC	*P* value	$\log_2$ FC	*P* value
PYL	XLOC_001385	−2.14	1.00^{ns}	3.05	1.00^{ns}
	XLOC_003186	−0.61	0.44^{ns}	0.36	0.72^{ns}
	XLOC_006253	−0.37	0.55^{ns}	1.70	0.00***
	XLOC_006910	−0.08	0.92^{ns}	0.55	0.29^{ns}
	XLOC_014772	−0.06	0.97^{ns}	1.76	0.01**
	XLOC_014773	−0.02	0.98^{ns}	0.64	0.22^{ns}
	XLOC_018382	0.27	0.64^{ns}	0.95	0.01**
	XLOC_019042	1.47	1.00^{ns}	4.69	0.00***
	XLOC_025240	1.83	0.01*	3.06	0.00***
PP2C	XLOC_002375	−0.41	0.69^{ns}	2.85	0.00***
	XLOC_002874	−0.09	0.90^{ns}	0.12	0.85^{ns}
	XLOC_002875	−0.03	0.98^{ns}	−0.49	0.55^{ns}
	XLOC_003308	0.03	0.97^{ns}	0.43	0.46^{ns}
	XLOC_003806	0.21	0.74^{ns}	0.05	0.95^{ns}
	XLOC_008259	0.53	0.58^{ns}	2.11	0.00***
	XLOC_014108	0.55	0.40^{ns}	0.31	0.68^{ns}
	XLOC_014109	0.59	0.17^{ns}	1.56	0.00***
	XLOC_019574	0.74	0.14^{ns}	1.54	0.00***
	XLOC_023260	1.29	1.00^{ns}	1.30	0.12^{ns}
SnRK2	XLOC_003694	−0.59	0.62^{ns}	1.83	0.03*
	XLOC_008135	−0.42	0.54^{ns}	−4.16	0.02*

Table II-6. Continued.

		Pale green to reddish purple		Reddish purple to dark purple	
Annotation	Transcript ID	$\log_2$ FC	*P* value	$\log_2$ FC	*P* value
	XLOC_008364	−0.17	0.86^{ns}	0.03	0.98^{ns}
	XLOC_010843	−0.16	0.81^{ns}	1.09	0.00^{**}
	XLOC_010844	−0.06	0.98^{ns}	−0.08	0.97^{ns}
	XLOC_013509	−0.04	0.96^{ns}	0.01	0.98^{ns}
	XLOC_013510	−0.02	0.98^{ns}	0.48	0.51^{ns}
	XLOC_014716	0.13	0.93^{ns}	−0.46	0.71^{ns}
	XLOC_016371	0.13	0.84^{ns}	0.13	0.85^{ns}
	XLOC_016372	0.25	0.71^{ns}	0.07	0.94^{ns}
	XLOC_017765	0.31	0.79^{ns}	0.02	0.99^{ns}
	XLOC_022345	0.39	0.43^{ns}	0.18	0.79^{ns}
ABF	XLOC_001247	−0.87	0.28^{ns}	−0.03	0.98^{ns}
	XLOC_004834	−0.53	0.22^{ns}	−0.29	0.58^{ns}
	XLOC_006309	−0.49	0.43^{ns}	0.77	0.15^{ns}
	XLOC_006310	−0.34	0.81^{ns}	0.92	0.36^{ns}
	XLOC_007054	−0.20	0.80^{ns}	0.07	0.95^{ns}
	XLOC_008985	−0.17	0.79^{ns}	0.49	0.29^{ns}
	XLOC_009041	−0.16	0.91^{ns}	0.23	0.86^{ns}
	XLOC_011318	−0.15	0.88^{ns}	0.49	0.52^{ns}
	XLOC_012531	0.03	0.97^{ns}	0.42	0.40^{ns}
	XLOC_014966	0.07	0.96^{ns}	−0.84	0.41^{ns}
	XLOC_016006	0.36	0.68^{ns}	2.00	0.00^{***}
	XLOC_021956	0.80	0.23^{ns}	2.02	0.00^{***}

Table II-6. Continued.

		Pale green to reddish purple		Reddish purple to dark purple	
Annotation	Transcript ID	log_2 FC	*P* value	log_2 FC	*P* value
	XLOC_023170	0.85	0.07^{ns}	2.30	0.00***
	XLOC_025428	1.33	0.53^{ns}	0.58	0.77^{ns}
	XLOC_025429	0.12	0.00***	0.30	1.00^{ns}
TDR	XLOC_005581	0.40	0.51^{ns}	0.14	0.87^{ns}
	XLOC_008525	0.06	0.93^{ns}	0.05	0.95^{ns}
	XLOC_012094	0.68	0.09^{ns}	0.07	0.93^{ns}
	XLOC_012234	−1.47	0.00***	0.18	0.81^{ns}
	XLOC_012235	−0.51	0.33^{ns}	−0.45	0.45^{ns}
	XLOC_012336	−0.42	0.45^{ns}	−0.10	0.90^{ns}
	XLOC_020801	−0.58	0.55^{ns}	0.17	0.90^{ns}
	XLOC_020802	−1.58	0.12^{ns}	1.82	0.08^{ns}
	XLOC_022202	−1.32	0.01*	−0.43	0.58^{ns}
	XLOC_025201	0.25	1.00^{ns}	1.56	0.15^{ns}
MYB	XLOC_002719	0.00	1.00^{ns}	10.29	0.42^{ns}
	XLOC_004086	1.25	1.00^{ns}	5.66	0.00***
	XLOC_014424	3.01	0.30^{ns}	4.28	0.00***
	XLOC_014506	−0.54	0.56^{ns}	2.48	0.00***
	XLOC_016597	−0.82	0.32^{ns}	1.72	0.00***
	XLOC_024956	0.17	0.90^{ns}	−1.02	0.29^{ns}
bHLH	XLOC_007052	−0.27	0.64^{ns}	0.96	0.01**
	XLOC_020812	0.31	0.78^{ns}	−1.74	0.06^{ns}
WDR	XLOC_012742	−0.09	0.90^{ns}	0.72	0.06^{ns}

Table II-6. Continued.

		Pale green to reddish purple		Reddish purple to dark purple	
Annotation	Transcript ID	$\log_2$ FC	*P* value	$\log_2$ FC	*P* value
	XLOC_014007	–0.03	0.97^{ns}	0.46	0.33^{ns}

^{ns,*,**,***} Non-significant or significant at $P < 0.05$, 0.01, or 0.001, respectively.

PYL, pyrabactin resistance-like; PP2C, protein phosphatases type 2C; SnRK2, sucrose non-fermenting-1-related protein kinase 2; ABF, ABA-responsive element binding factor; TDR, SQUAMOSA-class MADS box transcription factor; MYB, myeloblastosis transcription factor; bHLH, basic helix-loop-helix transcription factor; WDR, β-transduction repeat transcription factor.

dihydroflavonol 4-reductase (DFR), anthocyanidin synthase (ANS), anthocyanin 3-*O*-glucosyltransferase (UFGT), and *O*-methyltransferase (OMT) (Fig. II-8) (Zifkin et al., 2012; Lu et al., 2003). These enzymes and their related genes in anthocyanin biosynthesis have been discovered in several plant species, including *Arabidopsis*, maize, grape, and petunia (Lepiniec et al., 2006), and the anthocyanin biosynthesis pathway was reported to be highly conserved in angiosperms (Ahn et al., 2015).

In the present study, 42 transcripts were annotated to encode 12 enzymes involved in anthocyanin biosynthesis: four *CHS*s, two *CHI*s, six *F3H*s, one *F3'H*, five *F3'5'H*s, six *DFR*s, three *ANS*s, five *UFGT*s, three *OMT*s, five *leucoanthocyanidin reductases* (*LAR*s), one *anthocyanidin reductase* (*ANR*), and one *anthocyanidin 3-O-glucoside 2'''O-xylosyltransferase* (*UGT79B1*) (Fig. II-9). Of the 25 significantly regulated transcripts, ten transcripts (one *CHS* [XLOC_000676], three *F3H*s [XLOC_021090, XLOC_021091, and XLOC_024962], two *F3'5'H*s [XLOC_023335 and XLOC_025538], one *DFR* [XLOC_017095], and three *UFGT*s [XLOC_000512, XLOC_001255, and XLOC_012011]) were up-regulated from pale green to dark purple stages, while another ten transcripts (two *CHS*s [XLOC_006462 and XLOC_011961], one *CHI* [XLOC_013011], three *F3H*s [XLOC_005654, XLOC_021089, and XLOC_024963], one *F3'H* [XLOC_006400], one *DFR* [XLOC_001004], and two *ANS*s [XLOC_024611 and XLOC_025532]) were up-regulated from reddish purple to dark purple stages (Table II-7). In addition, one *OMT* (XLOC_009548), three *LAR*s (XLOC_006876, XLOC_014163, and XLOC_020879), and one *ANR* (XLOC_018239) were down-regulated throughout the entire ripening stages (Table II-7).

The transcripts encoding CHS, CHI, and F3H, which produce common

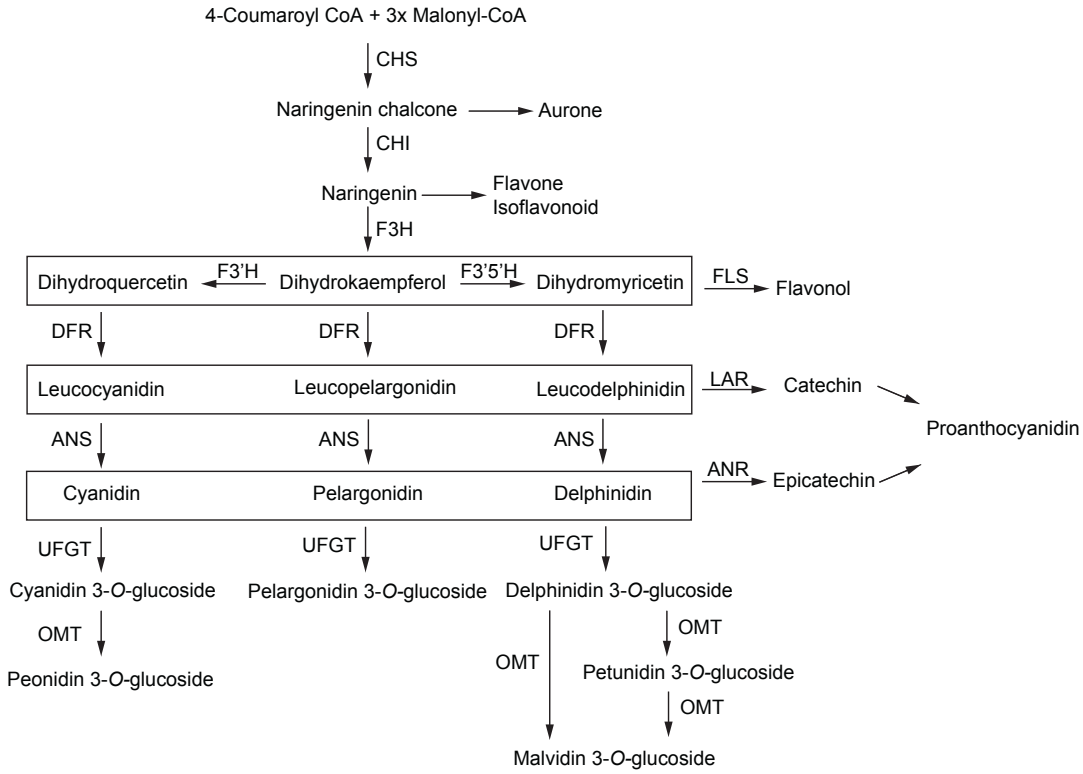

Fig. II-8. Schematic view of the anthocyanin biosynthesis pathway (modified from Zifkin et al. [2012]). CHS, chalcone synthase; CHI, chalcone isomerase; F3H, flavanone 3-hydroxylase; F3'H, flavonoid 3'-hydroxylase; F3'5'H, flavonoid 3',5'-hydroxylase; DFR, dihydroflavonol 4-reductase; ANS, anthocyanidin synthase; UFGT, anthocyanin 3-*O*-glucosyltransferase; OMT, *O*-methyltransferase; FLS, flavonol synthase; LAR, leucoanthocyanidin reductase; ANR, anthocyanidin reductase.

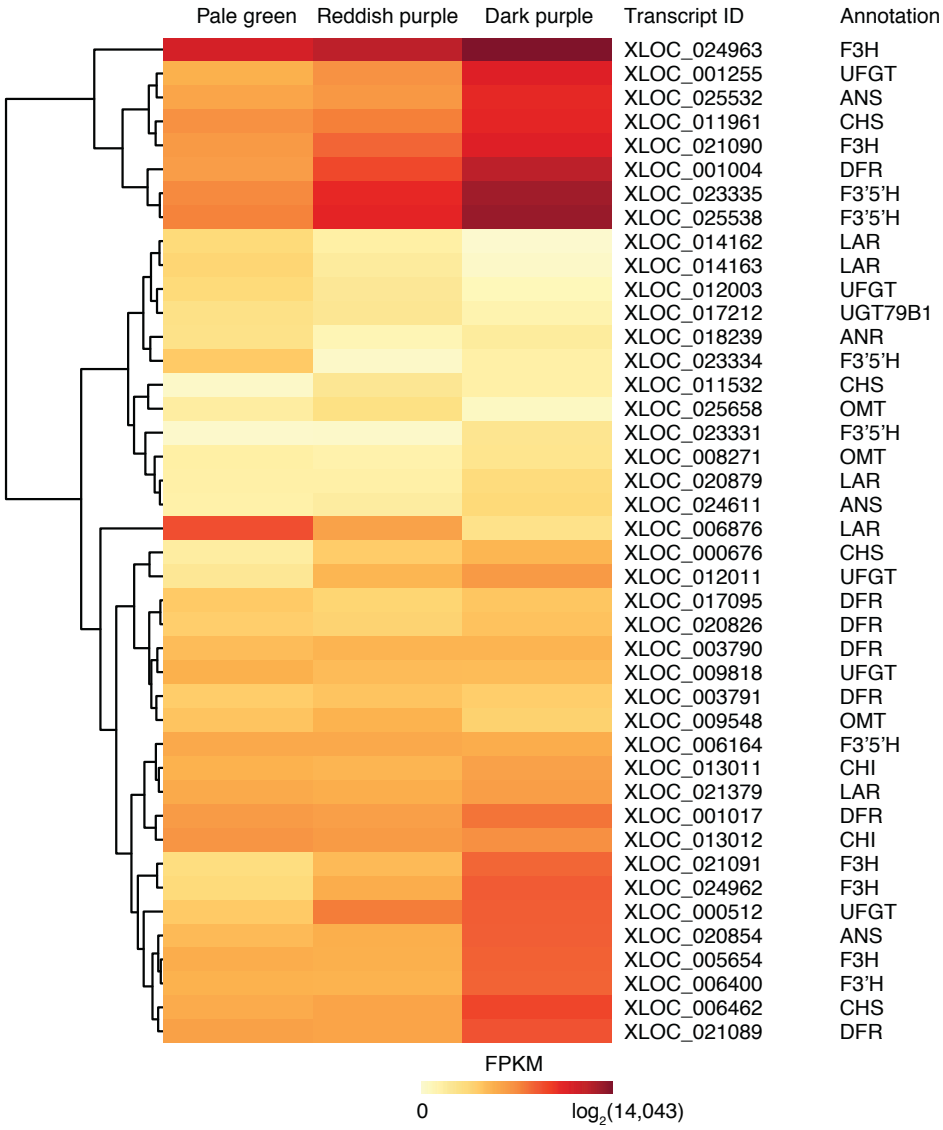

Fig. II-9. Heatmap of the $\log_2$ FPKM expression of candidate transcripts involved in anthocyanin biosynthesis in 'Bluecrop' highbush blueberry fruit during ripening. Three ripening stages based on fruit skin coloration: pale green at ca. 30 days after full bloom (DAFB), reddish purple at ca. 40 DAFB, and dark purple at ca. 50 DAFB. The differentially expressed genes were clustered based on their FPKM values. CHS, chalcone

synthase; CHI, chalcone isomerase; F3H, flavanone 3-hydroxylase; F3'H, flavonoid 3'-hydroxylase; F3'5'H, flavonoid 3',5'-hydroxylase; DFR, dihydroflavonol 4-reductase; ANS, anthocyanidin synthase; UFGT, anthocyanin 3-*O*-glucosyltransferase; OMT, *O*-methyltransferase; FLS, flavonol synthase; LAR, leucoanthocyanidin reductase; ANR, anthocyanidin reductase.

anthocyanin precursors (Fig. II-8), were all up-regulated throughhout the entire ripening stages (Table II-7), as observed in peach (Cao et al., 2017), sweet cherry (Shen et al., 2014), bilberry (Jaakola et al., 2010), and 'Rubel' highbush blueberry fruit (Zifkin et al., 2012).

The cytochrome P450-dependent monooxygenases F3'H and F3'5'H determine the types of anthocyanins (Seitz et al., 2015; Chapple, 1998). The F3´H and F3'5'H hydroxylate the B-ring of anthocyanidin skeletons at the 3'-, and 3'- and 5'-positions, respectively. The F3'H and F3'5'H are associated with the accumulations of cyanidin and delphinidin derivatives, respectively (Fig. II-8). Cyanidin and its methoxylated derivative peonidin confers red colors, while delphinidin and its methoxylated derivatives petunidin and malvidin are the main contributors of purple and blue colors (Hugueney et al., 2009). The anthocyanins except pelargonidins were abundantly found in ripe fruit of highbush blueberry (Chung et al., 2016; Kalt et al., 1999). In the present study, the two *F3'5'H*s (XLOC_023335 and XLOC_025538) were more highly expressed than *F3'H* (XLOC_006400) (Fig. II-9). The higher expression of *F3'5'H* than *F3'H* was consistent with the higher accumulation of the delphinidin derivatives than those of the cyanidin derivatives in several highbush blueberry cultivars (Chung et al., 2016; Kalt et al., 1999). Since an increase in the number of hydroxyl groups increases the blueness of the anthocyanins (Chapple, 1998; Hugueney et al., 2009), the expressions of the *F3'H* and *F3'5'H* (Fig. II-9) might lead to purple or blue skin coloration in 'Bluecrop' highbush blueberry fruit during ripening (Fig. II-1).

Following the hydroxylation, individual anthocyanins are biosynthesized at different levels depending on the reactions of DFR and ANS with their respective substrates (Lepiniec et al., 2006; Lu et al., 2003). In strawberry fruit, one DFR

Table II-7. Fold changes (FC) in the transcriptional expression involved in anthocyanin biosynthesis in 'Bluecrop' highbush blueberry fruit during ripening.

		Pale green to reddish purple		Reddish purple to dark purple	
Annotation	Transcript ID	$\log_2$ FC	*P* value	$\log_2$ FC	*P* value
CHS	XLOC_000676	2.82	0.00^{***}	0.97	0.04^{*}
	XLOC_006462	0.41	0.47^{ns}	3.14	0.00^{***}
	XLOC_011532	4.50	0.54^{ns}	−1.11	0.30^{ns}
	XLOC_011961	0.55	0.40^{ns}	2.97	0.00^{***}
CHI	XLOC_013011	−0.14	0.87^{ns}	0.94	0.04^{*}
	XLOC_013012	−0.25	0.66^{ns}	0.50	0.27^{ns}
F3H	XLOC_005654	−0.13	0.86^{ns}	2.92	0.00^{***}
	XLOC_021089	−0.11	0.91^{ns}	2.80	0.00^{***}
	XLOC_021090	1.71	0.00^{***}	2.49	0.00^{***}
	XLOC_021091	1.90	0.01^{**}	3.23	0.00^{***}
	XLOC_024962	2.21	0.00^{**}	2.95	0.00^{***}
	XLOC_024963	0.96	0.23^{ns}	1.72	0.01^{***}
F3'H	XLOC_006400	−0.06	0.94^{ns}	2.99	0.00^{***}
F3'5'H	XLOC_006164	−0.02	0.98^{ns}	−0.17	0.80^{ns}
	XLOC_023331	1.16	1.00^{ns}	4.83	0.55^{ns}
	XLOC_023334	−6.35	0.42^{ns}	3.14	1.00^{ns}
	XLOC_023335	3.03	0.00^{***}	2.90	0.00^{***}
	XLOC_025538	3.11	0.00^{***}	2.86	0.00^{***}
DFR	XLOC_001004	−0.22	0.71^{ns}	1.57	0.00^{***}
	XLOC_001017	0.38	0.68^{ns}	0.01	0.99^{ns}
	XLOC_003790	0.42	0.67^{ns}	−0.46	0.63^{ns}

Table II-7. Continued.

		Pale green to reddish purple		Reddish purple to dark purple	
Annotation	Transcript ID	$\log_2$ FC	*P* value	$\log_2$ FC	*P* value
	XLOC_003791	−0.65	0.42^{ns}	0.81	0.31^{ns}
	XLOC_017095	2.83	0.00***	3.18	0.00***
	XLOC_020826	−0.28	0.71^{ns}	0.88	0.07^{ns}
ANS	XLOC_020854	0.52	0.36^{ns}	2.95	0.00**
	XLOC_024611	0.60	0.80^{ns}	2.02	0.14^{ns}
	XLOC_025532	0.67	0.18^{ns}	3.67	0.00***
UFGT	XLOC_000512	3.21	0.00***	0.95	0.04*
	XLOC_001255	1.51	0.00**	3.90	0.00***
	XLOC_009818	−0.50	0.40^{ns}	−0.02	0.98^{ns}
	XLOC_012003	−1.45	0.19^{ns}	−2.32	0.31^{ns}
	XLOC_012011	3.15	0.00***	1.36	0.00**
UGT75B1	XLOC_017212	−0.54	0.54^{ns}	−1.66	0.13^{ns}
OMT	XLOC_008271	−0.44	1.00^{ns}	1.72	0.09^{ns}
	XLOC_009548	−0.73	0.00***	−1.42	0.01**
	XLOC_025658	1.49	0.05^{ns}	−4.05	0.09^{ns}
LAR	XLOC_006876	−2.81	0.00***	−3.52	0.00***
	XLOC_014162	−2.28	0.47^{ns}	0.75	0.12^{ns}
	XLOC_014163	−2.05	0.00***	−3.78	0.00***
	XLOC_020879	−0.02	0.00***	−2.14	0.00**
	XLOC_021379	−0.19	0.79^{ns}	0.75	0.09^{ns}
ANR	XLOC_018239	−2.66	0.02*	−1.53	0.00**

CHS, chalcone synthase; CHI, chalcone isomerase; F3H, flavanone 3-hydroxylase; F3’H,

flavonoid 3'-hydroxylase; F3'5'H, flavonoid 3',5'-hydroxylase; DFR, dihydroflavonol 4-reductase; ANS, anthocyanidin synthase; UFGT, anthocyanin 3-*O*-glucosyltransferase; UGT75B1, anthocyanidin 3-*O*-glucoside 2'''-*O*-xylosyltransferase; OMT, *O*-methyltransferase; LAR, leucoanthocyanidin reductase; ANR, anthocyanidin reductase.

isoform specifically reacted with dihydrokaempferol to biosynthesize pelargonidin derivatives, the most abundant anthocyanins in these fruit (Miosic et al., 2014).

Glucosylation, galactosylation, and arabinosylation were the major glycosylation processes, which were catalyzed by the actions of various sugar transferases, in highbush blueberry fruit (Chung et al., 2016; Oh et al., 2018). In our previous study, 22 anthocyanins resulted from these three glycosylation processes were determined in 'Bluecrop' highbush blueberry fruit (Chung et al., 2016). In the present study, however, three out of five transcripts encoding UFGTs for glucosylation were up-regulated throughout the entire ripening stages (Table II-7), but the transcripts associated with galactosylation and arabinosylation were not found (Fig. II-9). Similarly to this result, no transcripts associated with galactosylation or arabinosylation have been found in the other transcriptome analyses of highbush blueberry fruit (Gupta et al., 2015; Li et al., 2012; Li et al., 2016; Lin et al., 2018).

Leucoanthocyanidins and anthocyanidins can be diverted to flavan 3-ols by the actions of LAR and ANR, respectively (Zifkin et al., 2012). Since LAR and ANR compete with ANS and UFGT for their respective common substrates, the up-regulations of *ANS*s and *UFGT*s and the down-regulations of *LARs* and *ANR* (Table II-7) might also contribute to anthocyanin accumulation in highbush blueberry fruit during ripening. Following the glycosylation, OMT methoxylates the B-ring of anthocyanidin skeletons at the 3'-, and 3'- and 5'-positions (Jaakola et al., 2013; Lu et al., 2003). The transcript encoding OMT was found to be down-regulated in 'Bluecrop' highbush blueberry fruit throughout the entire ripening stages (Table II-7) as observed in grape fruit, despite of the accumulation of methoxylated anthocyanins (Hugueny et al., 2009).

Transcriptional expression in ABA-treated fruit

The effects of ABA treatment on the transcript expression were confirmed by qPCR analysis against the annotated transcripts, which were found to be highly up-regulated during ripening. All transcripts examined except for *CHI* (XLOC_013012) were more highly expressed in the ABA-treated fruit at 5 DAT than in untreated fruit (Fig. II-10). These included *NCED* (XLOC_002223), *TDR* (XLOC_020802), *CHS* (XLOC_011961), *F3H* (XLOC_024963), *F3'H* (XLOC_006400), *F3'5'H* (XLOC_025538), *DFR* (XLOC_001004), *ANS* (XLOC_025532), *UFGT* (XLOC_001255), and *OMT* (XLOC_008271).

The ABA-mediated up-regulation of *NCED* in 'Bluecrop' highbush blueberry fruit (Fig. II-10) was also previously observed in other non-climacteric fruits, including grape (Pilati et al., 2017), strawberry (Jia et al., 2011), and bilberry (Karppinen et al., 2018), implying that the endogenous ABA contents increased during ripening. Exogenous ABA as well as the increased endogenous ABA might accelerate the ripening process, including fruit skin coloration and cell softening.

The up-regulations of *TDR* and eight genes (*CHS*, *F3H*, *F3'H*, *F3'5'H*, *DFR*, *ANS*, *UFGT*, and *OMT*) (Fig. II-10) might contribute to the anthocyanin accumulation (Table II-2) and the associated fruit skin coloration (Fig. II-2, Table II-1). In ABA-treated grape (Koyama et al., 2018), strawberry (Jia et al., 2011), and blueberry fruits (Oh et al., 2018), however, the levels of anthocyanin accumulation and its associated gene expression were dependent on the concentration, timing, and duration of the ABA application. Despite these differences, the transcription factors and genes were similarly expressed in those fruits during ripening (Hu et al., 2018; Jia et al., 2011; Koyama et al., 2018; Oh et al., 2018). More detailed information on ABA effects under various environmental and experimental

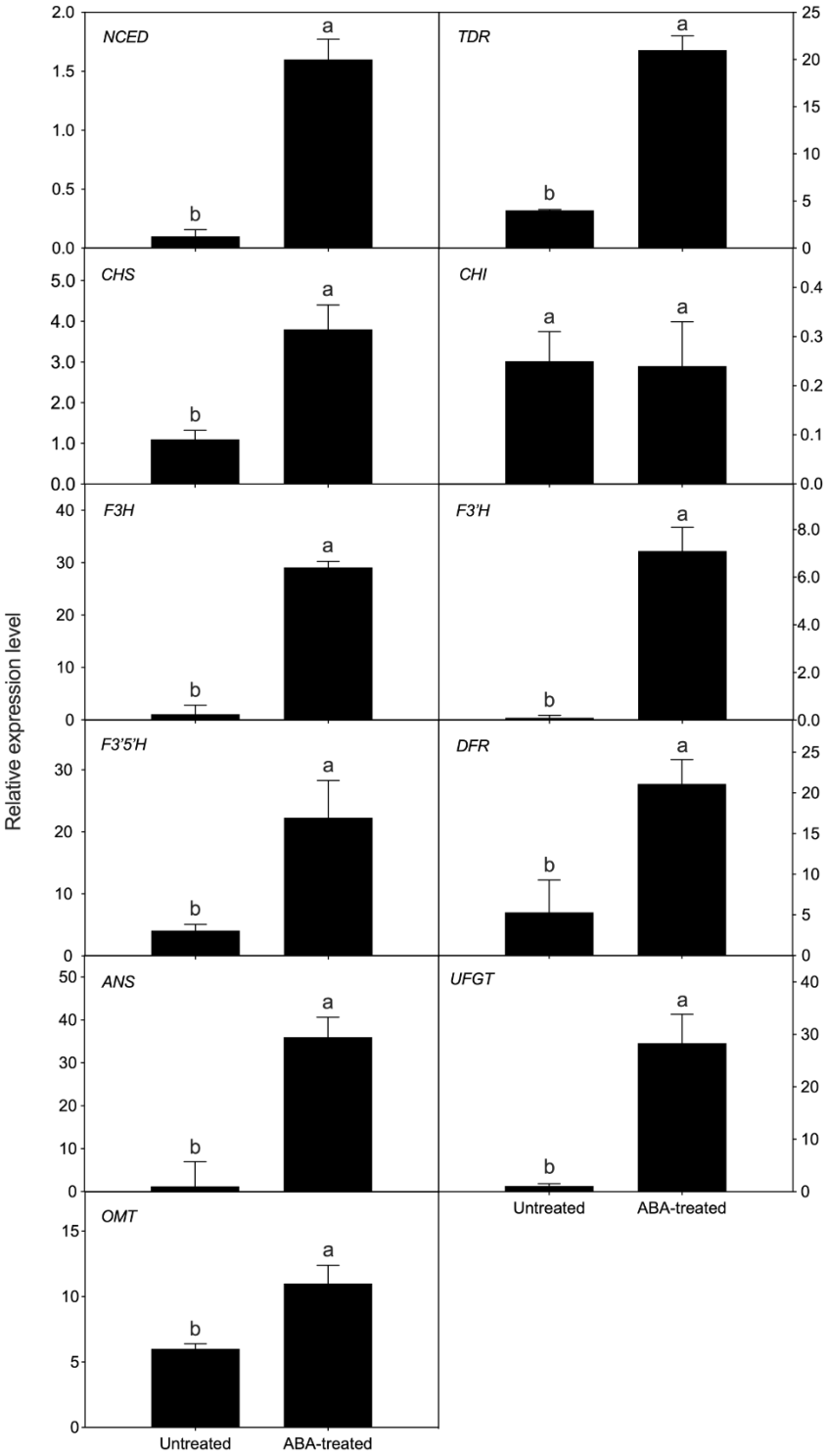
NCED
TDR
CHS
CHI
F3H
F3'H
F3'5'H
DFR
ANS
UFGT
OMT
Relative expression level
Untreated
ABA-treated

Fig. II-10. Relative gene expression in 'Bluecrop' highbush blueberry fruit at 5 days after treatment with or without 1 g L^{-1} (±) ABA at pale green stage (ca. 30 days after full bloom). Means within bars followed by different letters are significantly different according to Student's *t*-test at $P < 0.05$. Vertical bars represented standard errors of means (n = 3). *NCED*, nine-*cis*-epoxycarotenoid dioxygenase (XLOC_002223); *TDR*, SQUAMOSA-class MADS box transcription factor (XLOC_020802); *CHS*, chalcone synthase (XLOC_011961); *CHI*, chalcone isomerase (XLOC_013012); *F3H*, flavanone 3-hydroxylase (XLOC_024963); *F3'H*, flavonoid 3'-hydroxylase (XLOC_006400); *F3'5'H*, flavonoid 3',5'-hydroxylase (XLOC_025538); *DFR*, dihydroflavonol 4-reductase (XLOC_001004); *ANS*, anthocyanidin synthase (XLOC_025532); *UFGT*, anthocyanin 3-*O*-glucosyltransferase (XLOC_001255); *OMT*, *O*-methyltransferase (XLOC_008271).

conditions is needed to understand the ripening process of naturally grown fruits and to explore the possible implementation of ABA application in agricultural fields.

LITERATURE CITED

Ahn, J.H., J-S. Kim, S. Kim, H.Y. Soh, H. Shin, H. Jang, J.H. Ryu, A. Kim, K.Y. Yun, S. Kim, K.S. Kim, D. Choi, and J.H. Huh. 2015. De novo transcriptome analysis to identify anthocyanin biosynthesis genes responsible for tissue-specific pigmentation in zoysiagrass (*Zoysia japonica* Steud.). PLoS One 10: e0124497.

Ampomah-Dwamena, C., T. McGhie, R. Wibisono, M. Montefiori, R.P. Hellens, and A.C. Allen. 2009. The kiwifruit lycopene β-cyclase plays a significant role in carotenoid accumulation in fruit. J. Exp. Bot. 60: 3765–3779.

Cao, K., T. Ding, D. Mao, G. Zhu, W. Fang, C. Chen, X. Wang, and L. Wang. 2017. Transcriptome analysis reveals novel genes involved in anthocyanin biosynthesis in the flesh of peach. Plant Physiol. Biochem. 123: 94–102.

Chai, Y.M., H.F. Jia, C.L. Li, Q.H. Dong, and Y.Y. Shen. 2011. FaPYR1 is involved in strawberry fruit ripening. J. Exp. Bot. 62: 5079–5089.

Chapple, C. 1998. Molecular-genetic analysis plant cytochrome P450-dependent monooxygenases. Annu. Rev. Plant Physiol Plant Mol. Biol. 49: 311–343.

Chea, S., D.J. Yu, J. Park, H.D. Oh, S. W. Chung, and H.J. Lee. 2019. Fruit softening correlates with enzymatic and compositional changes in fruit cell wall during ripening in 'Bluecrop' highbush blueberries. Sci. Hortic. 245: 163–170.

Chen, J., L. Mao, W. Lu, T. Ying, and Z. Luo. 2016. Transcriptome profiling of postharvest strawberry fruit in response to exogenous auxin and abscisic acid. Planta 243: 183–197.

Chernys, J.T. and J.A. Zeevaart. 2000. Characterization of the 9-*cis*-epoxycarotenoid dioxygenase gene family and the regulation of abscisic acid

biosynthesis in avocado. Plant Physiol. 124: 343–353.

Chung, S.W., D.J. Yu, and H.J. Lee. 2016. Changes in anthocyanidin and anthocyanin pigments in highbush blueberry (*Vaccinium corymbosum* cv. Bluecrop) fruits during ripening. Hortic. Environ. Biotechnol. 57: 424–430.

Du, H., N. Wang, X. Li, J. Xio, and L. Xiong. 2010. Characterization of the β-carotene hydroxylase gene *DSM2* conferring drought and oxidative stress resistance by increasing xanthophylls and abscisic acid synthesis in rice. Plant Physiol. 154: 1304–1318.

Frenkel, C. 1972. Involvement of peroxidase and indole-3-acetic acid oxidase isoenzymes from pear, tomato, and blueberry fruit in ripening. Plant Physiol. 49: 757–763.

Gavrilova, V., M. Kajdzanoska, V. Gjamovski, and M. Stefova. 2011. Separation, characterization, and quantification of phenolic compounds in blueberries and red and black currants by HPLC-DAD-ESI-MS^n. J. Agric. Food Chem. 59: 4009–4018.

Giovannoni, J. 2001. Molecular biology of fruit maturation and ripening. Annu. Rev. Plant Physiol. 52: 725–749.

Gupta, V., A.D. Estrada, I. Blakley, R. Reid, K. Patel, M.D. Meyer, S.U. Andersen, A.F. Brown, M.A. Lila, and A.E. Loraine. 2015. RNA-Seq analysis and annotation of a draft blueberry genome assembly identifies candidate genes involved in fruit ripening, biosynthesis of bioactive compounds, and stage-specific alternative splicing. Gigascience 13: 5.

Hu, B., B. Lai, D. Wang, J. Li, L. Chen, Y. Qin, H. Wang, Y. Qin, G. Hu, and J. Zhao. 2019. Three LcABFs are involved in the regulation of chlorophyll degradation and anthocyanin biosynthesis during fruit ripening in *Litchi*

chinensis. Plant Cell Physiol. 60:448–461.

Hu, B., J. Li, D. Wang, H. Wang, Y. Qin, G. Hu, and J. Zhao. 2018. Transcriptome profiling of *Litchi chinensis* pericarp in respose to exogenous cytokinins and abscisic acid. Plant Growth Regul. 84:437–450.

Hugueney, P., S. Provenzano, C. Verries, A. Ferrandino, E. Meudec, G. Batelli, D. Merdinoglu, V. Cheynier, A. Schubert, and A. Ageorges. 2009. A novel cation-dependent *O*-methyltransferase involved in anthocyanin methylation in grapevine. Plant Physiol. 150: 2057–2070.

Jaakola, L. 2013. New insights into the regulation of anthocyanin biosynthesis in fruits. Trends Plant Sci. 18: 477–483.

Jaakola, L., A.M. Pirttila, M. Halonen, and A. Hohtola. 2001. Isolation of high quality RNA from bilberry (*Vaccinium myrtillus* L.) fruit. Mol. Biotechnol. 19: 201–203.

Jaakola, L., K. Maatta, A.M. Pirttila, R. Torronen, S. Karenlampi, and A. Hohtola. 2002. Expression of genes involved in anthocyanin biosynthesis in relation to anthocyanin, proanthocyanidin, and flavonol levels during bilberry fruit development. Plant Physiol. 130: 729–739.

Jaakola, L., M. Poole, M.O. Jones, T. Kamaraninen-Karppinen, J.J. Koskimaki, Hohtola A, H. Haggman, P.D. Fraser, K. Manning, G.J. King, H. Thomson, and G.B. Seymour. 2010. A SQUAMOSA MADS box gene involved in the regulation of anthocyanin accumulation in bilberry fruits. Plant Physiol. 153: 1619–1629.

Jeong, S.T., N. Goto-Yamamoto, S. Kobayashi, and M. Esaka. 2004. Effects of plant hormones and shading on the accumulation of anthocyanins and the expression of anthocyanin biosynthetic genes in grape berry skins. Plant Sci. 167: 247–252.

Jia, H.F., Y.M. Chai, C.L. Li, D. Lu, J.J. Luo, L. Qin, and Y.Y. Shen. 2011. Abscisic acid plays an important role in the regulation of strawberry fruit ripening. Plant Physiol. 157: 188–199.

Kalt, W., J.E. McDonald, R.D. Ricker, and X. Lu. 1999. Anthocyanin content and profile within and among blueberry species. Can. J. Plant Sci. 79: 617–623.

Karppinen, K., E. Hirvelä, T. Nevala, N. Sipari, M. Suokas, and L. Jaakola. 2013. Changes in the abscisic acid levels and related gene expression during fruit development and ripening in bilberry (*Vaccinium myrtillus* L.). Phytochemistry 95: 127–134.

Karppinen, K., P. Tegelberg, H. Haggman, and L. Jaakola. 2018. Abscisic acid regulates anthocyanin biosynthesis and gene expression associated with cell wall modification in ripening bilberry (*Vaccinium myrtillus* L.) fruits. Front. Plant Sci. 9: 1259.

Kondo, S., S. Meemak, Y. Ban, T. Moriguchi, and T. Harada. 2009. Effects of auxin and jasmonates on 1-aminocyclopropane-1-carboxylate (ACC) synthase and ACC oxidase gene expression during ripening of apple fruit. Postharvest Biol. Technol. 51: 281–284.

Koyama, K., K. Sadamatsu, and N. Goto-Yamamoto. 2010. Abscisic acid stimulated ripening and gene expression in berry skins of the Cabernet Sauvignon grape. Funct. Integr. Genom. 10: 367–381.

Koyama, R., S.R. Roberto, R.T. de Souza, W.F.S. Borges, M. Anderson, A.L. Waterhouse, D. Cantu, M.W. Fidelibus, and B. Blanco-Ulate. 2018. Exogenous abscisic acid promotes anthocyanin biosynthesis and increased expression of flavonoid synthesis genes in *Vitis vinifera* × *Vitis labrusca* table grapes in a subtropical region. Front. Plant Sci. 9: 323.

Lepiniec, L., I. Debeaujon, J.M. Routaboul, A. Baudry, L. Pourcel, N. Nesi, and M. Caboche. 2006. Genetics and biochemistry of seed flavonoids. Annu. Rev. Plant Biol. 57: 405–430.

Li, C., H. Jia, Y. Chai, and Y. Shen. 2011. Abscisic acid perception and signaling transduction in strawberry: a model for non-climacteric fruit ripening. Plant Signal Behav. 6: 1950–1953.

Li, D., Z. Luo, W. Mou, Y. Wang, T. Ying, and L. Mao. 2014. ABA and UV-C effects on quality, antioxidant capacity, and anthocyanin contents of strawberry fruit (*Fragaria ananassa* Duch.). Postharvest Biol. Technol. 90: 56–62.

Li, L., H. Zhang, Z. Liu, X. Cui, T. Zhang, Y. Li, and L. Zhang. 2016. Comparative transcriptome sequencing and de novo analysis of *Vaccinium corymbosum* during fruit and color development. BMC Plant Biol. 16: 223.

Li, X.Y., H.Y. Sun, J.B. Pei, Y.Y. Dong, F.W. Wang, H. Chen, Y. Sun, N. Wang, H. LI, and Y. Li. 2012. De novo sequencing and comparative analysis of the blueberry transcriptome to discover putative genes related to antioxidants. Gene 511: 54–61.

Lin, Y., Y. Wang, B. Li, H. Tan, D. Li, L. Li, X. Liu, J. Han, and X. Meng. 2018. Comparative transcriptome analysis of genes involved in anthocyanin synthesis in blueberry. Plant Physiol. Biochem. 127: 561–572.

Lu, Y. and M.D. Rausher. 2003. Evolutionary rate variation in anthocyanin pathway genes. Mol. Biol. Evol. 20: 1844–1853.

Lund, S., F. Peng, T. Nayar, K. Reid, and J. Schlosser. 2008. Gene expression analyses in individual grape (*Vitis vinifera* L.) berries during ripening initiation reveal that pigmentation intensity is a valid indicator of developmental staging within the cluster. Plant Mol. Biol. 68: 301–315.

Luo, H., S. Dai, J. Ren, C. Zhang, Y. Ding, Z. Li, Y. Sun, K. Ji, Y. Wang, Q. Li, P. Chen, C. Duan, Y. Wang, and P. Leng. 2014. The role of ABA in the maturation and postharvest life of a non-climacteric sweet cherry fruit. J. Plant Growth Regul. 33: 373–383.

McGuire, R.G. 1992. Reporting of objective color measurements. HortScience 27: 1254–1255.

Miosic, S., J. Thill, M. Milosevic, C. Gosch, S. Pober, C. Molito, S. Ejaz, A. Rompel, K. Stich, and H. Halbwirth. 2014. Dihydroflavonol 4-reductase genes encode enzymes with contrasting substrate specificity and show divergent gene expression profiles in *Fragaria* species. PLoS One 9: e112707.

Nambara, E. and A. Marion-Poll. 2005. Abscisic acid biosynthesis and catabolism. Annu. Rev. Plant Biol. 56: 165–185.

Oh, H.D., D.J. Yu, S.W. Chung, S. Chea, and H.J. Lee. 2018. Abscisic acid stimulates anthocyanin accumulation in 'Jersey' highbush blueberry fruits during ripening. Food Chem. 244: 403–407.

Ozsolak, F. and P.M.M. Milos. 2011. RNA sequencing: advances, challenges, and opportunities. Nat. Rev. Genet. 12: 87–98.

Park, S.Y., P. Fung, N. Nishimura, D.R. Jensen, H. Fujii, Y. Zhao, S. Lumba, J. Santiago, A. Rodrigues, T.F. Chow, S.E. Alfred, D. Bonetta, R. Finkelstein, N.J. Provart, D. Desveaux, P.L. McCourt, J.K. Zhu, J.I. Schroeder, B.F. Volkman, and S.R. Cutler. 2009. Abscisic acid inhibits type 2C protein phosphatases via the PYR/PYL family of START proteins. Science 324: 1068–1071.

Pilati, S., G. Bagagli, P. Sonego, M. Moretto, D. Brazzale, and G. Catorina. 2017. Abscisic acid is a major regulator of grape berry ripening onset: new insights into ABA signaling network. Front. Plant Sci. 8: 1093.

Rattanakon, S., R. Ghan, G.A. Gambetta, L.G. Deluc, K.A. Schlauch, and G.R. Cramer. 2016. Abscisic acid transcriptomic signaling varies with grapevine organ. BMC Plant Biol. 16: 72.

Ribera, A.E., M. Reyes-Diaz, M. Alberdi, G.E. Zuniga, and M.L. Mora. 2010. Antioxidant compounds in skin and pulp of fruits change among genotypes and maturity stages in highbush blueberry (*Vaccinium corymbosum* L.) grown in southern Chile. J. Soil Sci. Plant Nutr. 10: 509–536.

Rowland, L.J., N. Alkharoug, O. Darwish, E.L. OgdenL, L.O. Polashcok, N.V. Bassil, and D. Main. 2012. Generation and analysis of blueberry transcriptome sequences from leaves, developing fruit, and flower buds from cold acclimation through deacclimation. BMC Plant Biol. 12: 46.

Seitz, C., S. Ameres, K. Schlangen, G. Forkmann, and H. Halbwirth. 2015. Multiple evolution of flavonoid 3',5'-hydroxylase. Planta 242: 561–573.

Shen, X., K. Zhao, L. Liu, K. Zhang, H. Yuan, X. Liao, Q. Wang, X. Guo, F. Li, and T. Li. 2014. A role for PacMYBA in ABA-regulated anthocyanin biosynthesis in red-colored sweet cherry cv. Hong Deng (*Prunus avium* L.). Plant Cell Physiol. 55: 862–880.

Sun, L., Y. Sun, M. Zhang, L. Wang, J. Ren, M. Cui, Y. Wang, K. Ji, P. Li, Q. Li, P. Chen, S. Dai, C. Daun, Y. Wu, and P. Leng. 2012. Suppression of 9-*cis*-epoxycarotenoid dioxygenase, which encodes a key enzyme in abscisic acid biosynthesis, alters fruit texture in transgenic tomato. Plant Physiol. 158: 283–298.

Symons, G.M., Y.J. Chua, J.J. Ross, L.J. Quittenden, N.W. Davies, and J.B. Reid. 2012. Hormonal changes during non-climacteric ripening in strawberry. J. Exp. Bot. 63: 4741–4750.

Villalobos-González, L., A. Peña-Neira, F. Ibáñez, and C. Pastenes. 2016. Long-term effects of abscisic acid (ABA) on the grape berry phenylpropanoid pathway: gene expression and metabolite content. Plant Physiol. Biochem. 105: 213–223.

Wang, Z., M. Gerstein, and M. Snyder. RNA-Seq: a revolutionary tool for transcriptomics. 2009. Nat. Rev. Genet. 10: 57–63.

Wheeler, S., B. Loveys, C. Ford, and C. Davies. 2009. The relationship between the expression of abscisic acid biosynthesis genes, accumulation of abscisic acid, and the promotion of *Vitis vinifera* L. berry ripening by abscisic acid. Aust. J. Grape Wine Res. 15: 195–204.

Wu, X. and R.L. Prior. 2005. Systematic identification and characterization of anthocyanins by HPLC-ESI-MS/MS in common foods in the United States: fruits and berries. J. Agric. Food Chem. 53: 5789–5799.

Xu, F., S. Yuan, D.W. Zhang, X. Lv, and H.H. Lin. 2012. The role of alternative oxidase in tomato fruit ripening and its regulatory interaction with ethylene. J. Exp. Bot. 63: 5705–5716.

Yang, W., W. Zhang, and X. Wang. 2017. Post-transcriptional control of ABA signaling: the roles of protein phosphorylation and ubiquitination. Plant Biotechnol. J. 15: 4–14.

Young, P.R., J.G. Lashbrooke, E. Alexandersson, D. Jacobson, C. Moser, R. Velasco, and M.A. Vivier. 2012. The genes and enzymes of the carotenoid metabolic pathway in *Vitis vinifera* L. BMC Genom. 13: 243.

Zaharia, L.I., M.K. Walker-Simmon, C.N. Rodriguez, and S.R. Abrams. 2005. Chemistry of abscisic acid, abscisic acid catabolites, and analogs. J. Plant Growth Regul. 24: 274–284.

Zhang, M., B. Yuan, and P. Leng. 2009. The role of ABA in triggering ethylene

biosynthesis and ripening of tomato fruit. J. Exp. Bot. 60: 1579–1588.

Zifkin, M., A. Jin, J.A. Ozga, L.I. Zaharia, J.P. Schernthaner, A. Gesell, S.R. Abram, J.A. Kennedy, and C.P. Constabel. 2012. Gene expression and metabolite profiling of developing highbush blueberry fruit indicates transcriptional regulation of flavonoid metabolism and activation of abscisic acid metabolism. Plant Physiol. 158: 200–224.

CONCLUSIONS

The fruit coloration is the most important ripening process for plant survival. Non-climacteric blueberry fruit accumulate high levels of anthocyanins during ripening, leading to a highly noticeable coloration process. This ripening-related coloration makes blueberries suitable for studies of ripening.

During ripening of blueberry fruit, anthocyanin contents increased and various anthocynins were accumulated with skin coloration. The skin coloration was associated with athocyanindins, also called anthocyanin aglycones. In 'Bluecrop' highbush blueberry fruit, cyanidins, delphinidins, petunidins, malvidins, and peonidins were accumulated. Delphinidins, the predominant types of anthocyanin, were major determinants for the fruit skin coloration. These anthocyanidins were glycosylated with glucose, galactose, and arabinose, which might stabilize anthocyanin structure and enhane their colors. Abscisic acid (ABA) application in blueberry fruit accelerated the skin coloration and anthocyanin accumulation. These results suggested that the ripening of blueberry fruit is initiated by ABA, as observed in other non-climacteric fruits.

Transcriptome analysis revealed transcriptional regulation associated with ABA biosynthesis and signal transduction, and anthocyanin biosynthesis during ripening. Of 25,766 assembled transcripts, 143 were annotated to encode five ABA biosynthesis enzymes, four ABA signal transduction regulators, four ABA-responsive transcription factors, and 12 anthocyanin biosynthesis enzymes. After onset of ripening, some transcripts involved in ABA biosynthesis and signal transduction regulators, including *nine-cis-epoxycarotenoid dioxygenase* and *pyrabactin resistance*, were up-regulated during ripening. ABA-responsive

transcription factors, including SQUAMOSA MADS box which, were also up-reuglated, which trigger the expssion of genes encoding anthocyanin biosynthesis enzymes during ripening. Transcriptinonl regulation of anthocyanin biosynthesis might describe the highly accumulation of delphinidins in blueberry fruit, since *flavonoid 3',5'-hydorxylase* were more highly expressed than *flavonoid 3'-hydorxylase*.

ABSTRACT IN KOREAN

비급등형 과실로 알려진 블루베리(*Vaccinisum* spp.)는 숙성되는 동안 착색과 연관된 색소인 안토시아닌을 다량 축적한다. 본 연구에서는 '블루크랍' 하이부쉬 블루베리(*V. corymbosum*)를 대상으로 과실의 숙성에 영향을 미치는 신호 전달 기작과 과피 착색에 영향을 미치는 안토시아닌 생합성 과정을 구명하고자 하였다. 과실의 숙성 기간을 엷은 초록색(pale green, 만개 후 약 30일), 적자색(reddish purple, 만개 후 약 40일), 어두운 자주색(dark purple, 만개 후 약 50일)의 3단계로 나누어 과피 색의 변화, 안토시아니딘과 안토시아닌의 함량 변화를 측정하였다. 과실 숙성의 신호 기작인 앱시스산의 착색 효과를 확인하기 위해 1g L^{-1}의 앱시스산에 과방을 침지하였다. 이후 전사체 분석을 통해 앱시스산 생합성과 신호 전달 체계 및 안토시아닌 생합성 과정을 조사하였다. 블루베리 과실이 숙성됨에 따라 과피는 L*과 b* 값이 낮아졌으며, 총 안토시아닌 함량은 증가하였다. 블루베리 과실에서 5종류의 안토시아니딘이 발견되었다. 엷은 초록색 단계에서 시아니딘만 발견되었지만, 적자색 단계 이후에서는 시아니딘, 델피니딘, 말비딘, 피오니딘, 페투니딘이 발견되었다. 이 중 델피니딘과 말비딘의 함량이 가장 많았다. 5종류의 안토시아니딘들은 전부 글루코오스, 갈락토오스, 아라비노오스와 함께 글리코실화되었다. 앱시스산 처리는 과피 착색 및 안토시아닌 축적을 촉진시켰다. 전사체 분석 결과, 앱시스산 생합성, 신호 전달 및 안토시아닌 생합성에 관여하는 143개의 전사체를 확인하였다. 이중 *nine-cis-epoxycarotenoid dioxygenase*, *SQUAMOSA-class MADS box transcription factor*, *flavonoid 3',5'-hydroxylase*를 포함하는 11개의 전사체가 과실이 숙성하는 동안 발현량이 지속적으로

증가하였다. 과실이 숙성하는 동안 flavonoid 3',5'-hydroxylase의 전사체가 flavonoid 3′-hydroxylase의 전사체보다 많이 발현한 것은 델피니딘과 말비딘 계열의 안토시아닌 축적에 영향을 끼치기 때문인 것으로 판단되었다. 앱시스산을 처리한 블루베리 과실에서 *flavonoid 3',5'-hydroxylase*와 *flavonoid 3'-hydroxylase*를 포함한 9종류의 전사체를 대상으로 정량적 중합 효소 연쇄 반응을 시행한 결과, 과실 숙성 동안과 유사한 발현 양상을 보였다. 본 연구 결과는 앱시스산이 과실이 숙성하는 동안 과피 착색 및 안토시아닌 축적에 영향을 미치고, 안토시아닌 생합성 전사 인자 및 효소가 안토시아닌의 종류별 함량를 결정할 수 있음을 시사한다.